Molecular Biology of the Cell
Vol. 7, 1299–1317, August 1996

Nuclear Accumulation of Fibroblast Growth Factor Receptors Is Regulated by Multiple Signals in Adrenal Medullary Cells

Michal K. Stachowiak,*† Pamela A. Maher,‡ Anna Joy,* Eli Mordechai,* and Ewa K. Stachowiak*

*Barrow Neurological Institute, Phoenix, Arizona 85013; and ‡The Scripps Research Institute, La Jolla, California 92037

Submitted March 8, 1996; Accepted May 15, 1996
Monitoring Editor: Carl-Henrik Heldin

In an effort to determine the localization of fibroblast growth factor (FGF) receptors (FGFR) that could mediate the intracellular action of FGF-2, we discovered the presence of high-affinity FGF-2 binding sites in the nuclei of bovine adrenal medullary cells (BAMC). Western blot analysis demonstrated the presence of 103-, 118-, and 145-kDa forms of FGFR1 in nuclei isolated from BAMC. ^{125}I-FGF-2 cross-linking to nuclear extracts followed by FGFR1 immunoprecipitation showed that FGFR1 can account for the nuclear FGF-2 binding sites. Nuclear FGFR1 has kinase activity and undergoes autophosphorylation. Immunocytochemistry with the use of confocal and electron microscopes demonstrated the presence of FGFR1 within the nuclear interior. Nuclear subfractionation followed by Western blot or immunoelectron microscopic analysis showed that the nuclear FGFR1 is contained in the nuclear matrix and the nucleoplasm. Agents that induce translocation of endogenous FGF-2 to the nucleus (forskolin, carbachol, or angiotensin II) increased the intranuclear accumulation of FGFR1. This accumulation was accompanied by an overall increase in FGF-2–inducible tyrosine kinase activity. Our findings suggest a novel mode for growth factor action whereby growth factor receptors translocate to the nucleus in parallel with their ligand and act as direct mediators of nuclear responses to cell stimulation.

INTRODUCTION

According to the classical theory of signal transduction, the role of a membrane-associated growth factor receptor is to transmit signal from the extracellular environment to the cytoplasm. Other cytoplasmic proteins and kinases serve as second messengers and propagate the signal downstream to the nucleus. However, not all the biological effects of growth factors may be produced in this manner. In recent years, a number of laboratories have reported an association of peptide growth factors with the cell nucleus, suggesting that at least some of their biological effects are produced through a direct interaction with nuclear effectors (reviewed, Burwen and Jones, 1987; Jans, 1994). The pleiotropic proteins, fibroblast growth factor-1 (FGF-1)[1] and FGF-2, could act via such a mechanism. Both proteins lack the signal sequence typical of other secreted proteins (Abraham *et al.*, 1986a,b; Jaye *et al.*, 1986) and are found primarily cell-associated (Schweigerer *et al.*, 1987; Vlodawski *et al.*, 1991; Moscatelli, 1988, Stachowiak *et al.*, 1994). Consistent with the intracellular localization of FGFs are studies that show the following: 1) FGF-2 does not need to be

† Corresponding author: Laboratory of Molecular Neurobiology, Barrow Neurological Institute, 350 West Thomas Road, Phoenix, AZ 85013.

[1] Abbreviations used: BAMC, bovine adrenal medullary cells; BSA, bovine serum albumin; C-term FGFR1 Ab, C-terminal FGFR1 antibody; FGF, fibroblast growth factor; DSS, disuccinimidyl suberate; FGFR, fibroblast growth factor receptor; FGF-2-IF, FGF-2 immunofluorescence; FGFR1-IF, FGFR1 immunofluorescence; McAb6, monoclonal FGFR1 antibody; NLS, nuclear localization signal.

secreted to stimulate proliferation of fibroblasts (Bikfalvi *et al.*, 1995; Ray *et al.*, 1995) or differentiation of avian Schwann cells (Sherman *et al.*, 1993); 2) extracellularly added FGF-2 accumulates in the nucleus in a cell cycle-dependent manner (Baldin *et al.*, 1990); 3) FGF-2 added to isolated nuclei stimulates rRNA synthesis (Bouche *et al.*, 1987) and affects in vitro gene transcription in nuclear extracts (Nakanishi *et al.*, 1992); and 4) the mitogenic action of exogenous FGF-1 requires nuclear translocation of this protein (Imamura *et al.*, 1990; Wiedlocha *et al.*, 1994). Thus, FGFs may act as intracellular proteins, and some biological effects of FGFs may be produced directly in the nucleus.

FGFs interact with high-affinity tyrosine kinase receptors, which bind FGFs with picomolar affinity and are thought to mediate the cellular responses to FGFs, and low-affinity receptors, which bind FGFs with nanomolar affinity and are characterized by the presence of heparan sulfate (reviewed, Johnson and Williams, 1993; Wilkie *et al.*, 1995). Four genes are known to encode the high-affinity FGF receptors (FGFR), with multiple variants arising because of alternative splicing (Ruta *et al.* 1989; Dionne *et al.*, 1990; Keegan *et al.*, 1991; Partanen *et al.*, 1991). Each member of the FGFR gene family encodes an extracellular domain (N-terminal domain), which is composed of three immunoglobulin-like domains containing the growth factor binding region, a single transmembrane domain, and an intracellular domain with a split tyrosine kinase region (reviewed, Johnson and Williams, 1993). Although the biological effects of extracellular FGF-2 are thought to be mediated by the high-affinity cell surface receptors (reviewed, Mason, 1994), intracellular FGF-2 may stimulate cellular proliferation through mechanisms independent of the presence of a cell surface receptor (Bikfalvi *et al.*, 1995). Prudovsky *et al.* (1994) showed that cell surface FGFR1 redistributes to a cytoplasmic–perinuclear location after stimulation of cells by exogenous ligand. Fractionation of human glial cells revealed the presence of FGFR1 in the isolated nuclei (Stachowiak *et al.*, 1996) and its regulation in association with cell proliferation (Stachowiak *et al.*, unpublished data). The presence of FGF receptors (FGFR3) was also observed in the nuclei-containing subcellular fraction of breast cancer cells (Johnston *et al.*, 1995).

In the chromaffin cells of the adrenal medulla, the appearance of FGF-2 protein during development coincides with the establishment of functional innervation (Grothe and Unsicker, 1990) and can be induced in vitro by direct stimulation of acetylcholine receptors (Stachowiak *et al.*, 1994). These findings suggest that FGF-2 can serve as an intermediary in the neural regulation of adrenal medullary cells. Indeed, FGF-2 alters the expression of neurotransmitter biosynthetic genes in adrenal chromaffin cells (Puchacz *et al.*, 1993), promotes transmitter storage and synthesis (Unsicker and Westermann, 1992), and stimulates the proliferation of cultured chromaffin cells (Stemple *et al.*, 1988; Tischler *et al.*, 1993; Frodin and Gammeltoft, 1994).

In cultured bovine adrenal medullary cells (BAMC) the increases in the FGF-2 content evoked by the stimulation of neurotransmitter (acetylcholine) or hormonal (angiotensin II) receptors and their signaling pathways do not result in a detectable presence of FGF-2 outside the cells. Instead, FGF-2 accumulates in the nucleus (Puchacz *et al.*, 1993; Stachowiak *et al.*, 1994). The regulated targeting of endogenous FGF-2 to the nucleus suggests that this growth factor may serve as an intracrine nuclear-signaling molecule in adrenal medullary cells. In this study we show the nuclear presence of functional high-affinity FGF receptors (FGFR1) in adrenal medullary cells and their regulation by extrinsic molecules and intracellular signaling pathways. FGFR1 translocates to the nucleus in parallel with FGF-2. Our results suggest that FGFR1 could act as a nuclear mediator of the cellular response to trans-synaptic or hormonal stimulation.

MATERIALS AND METHODS

Materials

Culture media were from Grand Island Biologicals (Grand Island, NY). The remaining reagents were from Boehringer Mannheim (Indianapolis, IN), Sigma Chemical (St. Louis, MO), Bio-Rad (Richmond, CA), Stratagene (La Jolla, CA), DuPont NEN (Boston, MA), Pharmacia (Alameda, CA); Santa Cruz Biotechnology (Santa Cruz, CA), Genzyme (Cambridge, MA) and Pierce (Rockford, IL).

Adrenal Medullary Cell Culture and Cell Fractionation

Chromaffin cells from bovine adrenal medullae (BAMC) were prepared by collagenase digestion (Stachowiak *et al.*, 1990) and purified by density gradient centrifugation in Renografin as described elsewhere (Puchacz *et al.*, 1993). Cells were plated in 30-mm wells (4×10^6 cells/well) and maintained in DMEM/F-12 medium containing 10% fetal calf serum for 2–3 d. Drug treatment was initiated after cells were in serum-free medium supplemented with fatty acid-free bovine serum albumin (0.1 mg/ml) for 40–48 h (Stachowiak *et al.*, 1994). Forskolin and phorbol 12-myristate 13-acetate (PMA) were added with 0.007% dimethyl sulfoxide (DMSO) as the vehicle. Control cells received 0.007% DMSO. Carbachol and the stable angiotensin II analogue, sar^1-angiotensin II, were dissolved in medium.

Cell fractionation was performed by the hypotonic/NP-40 lysis method of Schreiber *et al.* (1989) or the isotonic method of Boyle *et al.* (1985). In the hypotonic protocol, cells were washed in Tris-buffered saline (TBS), swollen in homogenization buffer containing (in mM): 10 HEPES, pH 7.9, 10 KCl, 0.1 EDTA, 0.1 ethylene glycol-bis(β-aminoethyl ether)-*N,N,N′,N′*-tetraacetic acid (EGTA), 1 dithiothreitol (DTT), and 0.5 phenylmethylsulfonyl fluoride (PMSF) and vortexed in homogenization buffer containing 0.6% NP-40. Nuclei were pelleted by centrifugation for 30 s in a microfuge and washed in homogenization buffer containing NP-40. The nuclear pellet and supernatant containing cytoplasm and plasma membranes were used for further analyses. Isotonic lysis of cells, isolation of nuclei and cytoplasmic fractions, and subfractionation of the nuclei were performed as described by Boyle *et al.* (1985) with minor modifications (Stachowiak *et al.*, 1994, 1996). Cells were incubated in isotonic

nuclear buffer containing 0.1% digitonin, 5 mM sodium phosphate, pH 7.4, 50 mM NaCl, 150 mM sucrose, 5 mM KCl, 2 mM dithiothreitol, 1 mM $MgCl_2$, 0.5 mM $CaCl_2$, 0.1 mM PMSF, 10 μM leupeptin, 1 μg/ml aprotinin, 25 μg/ml soybean trypsin inhibitor, and 5 μg/ml pepstatin A; cell lysates were collected by scraping. Nuclei were collected by centrifuging at 500 × *g* for 10 min at 4°C. The postnuclear supernatant was further centrifuged at 40,000 × *g* for 30 min at 4°C, and the supernatant was reserved for analysis of cytoplasmic FGFR. The crude nuclear pellet was resuspended in nuclear buffer and further purified by centrifugation through a cushion of TN buffer (2.5 mM Tris-HCl, pH 7.4, and 10 mM NaCl) containing 30% sucrose at 1000 × *g* for 10 min at 4°C. The isolated nuclei were washed twice in the isotonic nuclear buffer. The nuclei isolated by this method contain nearly 90% of the total TCA-precipitable DNA (Stachowiak *et al.*, 1996). The purity of isolated fractions was evaluated by measuring the activity of plasma membrane 5'-nucleotidase and lysosomal acid phosphatase with Sigma assay kits, as suggested by the manufacturer.

Further subfractionation of the nuclei isolated by the isotonic lysis method was performed according to Boyle *et al.* (1985), as described in Stachowiak *et al.* (1996). Briefly, to release nucleoplasm, 0.5–1.0 × 10^6 isolated nuclei were incubated for 30 min in 1 ml of NP-40 buffer (10 mM sodium phosphate, pH 7.4, 120 mM NaCl, and 0.5% NP-40). Post-NP-40 nuclei were collected by centrifuging for 10 min at 1000 × *g*. The extraction of nucleoplasm was repeated twice more, and the combined supernatants were used as the nucleoplasmic fraction. To release DNA and chromatin-associated proteins, NP-40 pellets were suspended in 100 μl of nuclease digestion buffer (20 mM Tris-HCl, pH 7.4, 100 mM NaCl, 50 mM KCl, 5 mM $CaCl_2$, 0.1 mM EDTA, 0.1 mM PMSF, and 170 U/ml micrococcal nuclease) and incubated for 30 min at 37°C. High salt buffer (900 μl, 2 M NaCl, 0.5% NP-40, 5 mM sodium phosphate, pH 7.4, and 10 mM EDTA) was added, and samples were incubated for 30 min on ice. The released material was separated from the pellet by centrifuging over a cushion of TN buffer containing 30% sucrose at 12,000 × *g* for 15 min. The supernatant (chromatin-binding fraction) was removed, and the insoluble pellet (nuclear matrix) was redigested and re-extracted with high salt buffer and collected by centrifugation as before. Supernatants containing the chromatin-binding fraction were combined. All samples were frozen in liquid nitrogen and stored at −80°C until use. The nuclear matrix–lamina complex isolated as described above contained 1–3% of the total precipitable nuclear DNA (A. Joy and M.K. Stachowiak, unpublished data). By the criterion of colocalization of core histones and DNA, treatment with nuclease and high salt efficiently released chromatin-associated proteins and DNA, leaving the nuclear matrix–lamina complex. Electron microscopy showed the absence of nuclear membrane and contaminating cytoplasmic organelles in the nuclear matrix fraction. The purity of chromatin fraction was evaluated by polyacrylamide gel-electrophoresis and silver staining for detection of core histones. Proteins with the same apparent molecular weight (12–18 kDa) as the core histones were detected only in the chromatin fraction (A. Joy and M.K. Stachowiak, unpublished data).

Binding of ^{125}I-Human Recombinant FGF-2 to the Cell Surface and to Nuclear and Cytoplasmic Fractions of BAMC

Nuclei and cytoplasmic fractions were isolated as described above. The binding of ^{125}I-FGF-2 was examined via the method of Moscatelli *et al.* (1987). Cells were plated overnight at 1 × 10^6/well in 12-well plates in serum-free Eagle's minimum essential medium (MEM) containing 0.15% gelatin. Subsequently, cells were washed twice with ice-cold phosphate-buffered saline (PBS) and were incubated for 4 h at 4°C in 100 μl of MEM containing 25 mM HEPES, 0.15% gelatin, and increasing concentrations (0–50 nM) of ^{125}I-FGF-2 (specific activity 70 uCi/μg) with or without a 100-fold molar excess of unlabeled FGF-2. Cells were washed three times with PBS, and the low-affinity binding fraction was extracted with 1 ml of 2 M NaCl in 20 mM HEPES, pH 7.5. The high-affinity binding fraction was obtained by solubilizing the cells in 250 μl of 0.5% Triton X-100 in 0.1 M sodium phosphate, pH 8.1. Each fraction was counted for ^{125}I-FGF-2 by using a Tracor Gamma counter. Nuclear and cytoplasmic fractions were collected from 10^6 cells and diluted with a binding buffer (25 mM HEPES, pH 7.5, and 0.15% gelatin) and 0–50 nM ^{125}I-FGF-2. The binding was performed in suspension at room temperature for 2 h in gently rotating tubes in the presence or absence of a 100-fold excess of unlabeled FGF-2. The reaction mixtures were transferred to Amicon-50 microconcentrators and centrifuged 10 min, 6000 × *g*, at room temperature. The filter-retained fraction of ^{125}I-FGF-2 was counted and analyzed by the Mac Ligand program.

Western Blot Analysis of FGFR in Subcellular Fractions

Western analysis of FGFR1 was performed as described in Stachowiak *et al.* (1996). Briefly, protein concentrations were determined by the Bio-Rad protein assay. Equal amounts of proteins from the cytoplasmic, membrane, and nuclear fractions (50 μg) were solubilized in 2.5× SDS-sample buffer and separated on SDS-7.5% polyacrylamide gel and transferred to nitrocellulose. The transfers were stained with amido black to confirm the presence of equal amounts of protein in each lane. Blots were probed by the use of polyclonal affinity-purified rabbit antibody to the carboxyl terminus of FGFR1 (C-term FGFR1 Ab; Hanneken *et al.*, 1995). The C-term FGFR1 Ab does not cross-react with FGFR2, FGFR3, or FGFR4 (Hanneken *et al.*, 1995). The second antibody used was the monoclonal antibody (McAb6) against the extracellular domain of FGFR1 produced in baculovirus that was characterized in Hanneken *et al.* (1995). Nitrocellulose membranes were blocked with 0.1% Tween 20 (C-term FGFR1 Ab) or 5% nonfat milk (McAb6) in TBS overnight before incubation with antibodies. Transfers were incubated with C-term FGFR1 Ab (2 μg/ml) for 4 h, washed, and then treated with ^{125}I-labeled protein A (0.2 uCi/ml). For McAb6, the transfers were incubated overnight with the antibody (3 μg/ml), washed, and then incubated with 1 μg/ml of rabbit anti-mouse immunoglobulin (IgG) for 2 h before ^{125}I-protein A was added, as described above. The transfers were autoradiographed overnight at −70°C. Apparent molecular sizes of FGFR forms were determined by comparison with concurrently run protein molecular weight standards. FGFR1 protein levels in the fractions were estimated by densitometric scanning of autoradiograms with a Beckman DU70 spectrophotometer.

Receptors in soluble subnuclear fractions (chromatin or nucleoplasm) were concentrated by overnight absorption to WGA-Sepharose (Pharmacia) at 4°C. The precipitates were washed twice with 0.1% Triton X-100 in 20 mM HEPES, pH 7.5, and 150 mM NaCl, and once with PBS before elution with 2.5× SDS-sample buffer. The nuclear matrix pellet was dissolved directly in 2.5× SDS-sample buffer. Western analysis of subnuclear fractions was performed as described for subcellular fractions.

Cross-linking of ^{125}I-FGF-2 to Receptors and Immunoprecipitation of Cross-linked FGFR

^{125}I-FGF-2 was prepared as described, using lactoperoxidase (Schubert *et al.*, 1987). The free iodine was separated from the iodinated growth factor by passage over a heparin-Sepharose column. Specific activity was 4–6 × 10^5 cpm/ng. Nuclear extracts were prepared by sonicating isolated nuclei in 1.0% Triton X-100 buffer containing (in mM): 50 HEPES, pH 7.5, 50 NaCl, 5 EDTA, and 1 Na_3Vo_4. For cross-linking, cells, nuclear extracts, or cytoplasmic fractions were incubated with 10^6 cpm/ml of ^{125}I-FGF-2 in 150 mM NaCl and 20 mM HEPES, pH 7.5, for 2 h with rotation at 4°C. Samples were rinsed twice with PBS and incubated with 0.15 mM disuccinimidyl suberate (DSS; Pierce) in PBS for 15 min at room temperature (cell surface receptors), or at 37°C (nuclear and cytoplasmic receptors)

with rotation. The cross-linking was stopped by the addition of 200 mM ethanolamine. The samples were rinsed twice with PBS and then solubilized in 500 μl of Triton X-100 buffer. FGFR were immunoprecipitated at 4°C overnight with antibodies against the C-terminal domains of the different types of FGFR (FGFR1, 2, 3, or 4; Santa Cruz Biotechnology) as described below. The immunoprecipitates were collected on protein A-Sepharose, washed twice with 0.1% Triton X-100 buffer in 20 mM HEPES, pH 7.5, and 150 mM NaCl, once with PBS, and solubilized in SDS-sample buffer. The samples were separated on SDS-7.5% polyacrylamide gels, and the gels were dried and autoradiographed.

Immunoprecipitation of FGF and In Vitro Kinase Assays

Nuclear proteins were solubilized by sonication of isolated nuclei in Triton X-100 buffer to give a final protein concentration of 1 mg/ml. FGFR were immunoprecipitated at 4°C overnight with the commercial anti-FGFR1 antibody (0.5 μg/500 μl nuclear extract; Santa Cruz Biotechnology) and the immunoprecipitates were collected on protein A-Sepharose, washed three times with 0.1% Triton X-100 in 20 mM HEPES, pH 7.5, 150 mM NaCl, 10% glycerol, and 1 mM Na_3VO_4, and resuspended in 50 μl of in vitro phosphorylation buffer (150 mM NaCl, 20 mM HEPES, pH 7.5, and 0.1% Triton X-100) containing 10 mM $MnCl_2$, 50 mM $MgCl_2$, 50 nM ATP, and 10 uCi [gamma-^{32}P]ATP. The reaction was performed for 20 min at room temperature with continuous rotation and then terminated by the addition of an equal volume of 5× SDS-sample buffer. The samples were separated on SDS-7.5% polyacrylamide gels, and the gels were fixed overnight in 25% methanol and 10% acetic acid, dried, and autoradiographed for 12–18 h.

Protein tyrosine kinase activity in nuclei was assayed as described (Maher, 1991) with poly glu/tyr (4:1) as substrate. The reactions were analyzed by SDS-polyacrylamide gel electrophoresis and autoradiography, after which the substrate bands were cut from the gel and the incorporation of ^{32}P was quantified by Cerenkov counting.

Immunohistochemical Staining

Cultured cells were fixed, permeabilized with 1% Triton X-100, and stained immunohistochemically as described previously (Stachowiak *et al.*, 1994, 1996), using the same FGFR1 antibodies (C-term FGFR1 Ab or McAb6; Hanneken *et al.*, 1995) that were used in Western blot assays. Fluorescent staining of FGFR1 immune complexes was performed with CY^3- or rhodamine-conjugated secondary antibodies (for C-term FGFR1 Ab) or Cy^5-conjugated goat anti-mouse IgG (for McAb6) (Jackson ImmunoResearch Labs, West Grove, PA). Digitized images of 1-μm confocal optical sections were acquired with a Bio-Rad MRC 600 confocal microscope with YHS 568 nm (Cy^3) or RHS (Cy^5) filter blocks and a 15 mW Krypton/Argon laser (see Figures 4, 7B, and 8C) or with a Carl Zeiss Laser Confocal Scanning Microscope 410 (see Figure 7A). Rhodamine epifluorescence was observed and photographed also under a conventional fluorescence microscope (see Figure 8).

The specificity of FGFR1 immunostaining was indicated by several observations: 1) Staining was not observed when the primary antibody was omitted or replaced with preimmune serum; 2) Similar staining was observed by using two different antibodies (C-term FGFR1 Ab and McAb6) and different staining techniques; 3) The same staining technique detected FGFR1 in the nuclei and the cytoplasmic enzyme tyrosine hydroxylase in the cytoplasm (our unpublished observations); 4) Neutralization of the C-term FGFR1 Ab by an excess of the C-terminal FGFR1 peptide reduced cytoplasmic FGFR1 staining and eliminated nuclear FGFR1 staining; and 5) The presence and changes in the levels of nuclear FGFR1 immunoreactivity were confirmed by Western blot analysis of FGFR1 in subcellular fractions.

FGF-2 was detected by using monoclonal FGF-2 antibody (UBI, Lake Placid, NY) and Cy^5-conjugated goat anti-mouse IgG. The specificity of FGF-2 staining was shown in Puchacz *et al.* (1993) and Stachowiak *et al.* (1994, 1996). Colocalization of FGFR1 and FGF-2 was examined by incubating fixed BAMC with polyclonal C-term FGFR1 Ab and monoclonal FGF-2 Ab. The immune complexes were stained with Cy^5-goat anti-rabbit IgG (FGFR1) and Cy^3-goat anti-mouse IgG (FGF-2). The Cy^5 was exited at 568 nm and Cy^3 at 647 by using YHS and RHS filter blocks, respectively. The two images were collected by using the same Z values and were merged.

Immunoelectron Microscopy

Cells were fixed for 15 min in 2% formaldehyde and 0.5% glutaraldehyde in PBS at room temperature. Postfixation with 1% osmium tetroxide greatly reduced immunostaining and therefore was not used. Without osmium postfixation the overall cell structure was retained, but, at higher magnification, regions of cytoplasm showed some disruption. After fixation, samples were washed three times in distilled water, 10 min each, and dehydrated through an ethanol series, 30, 50, 70, 80, and 90% for a minimum of 10 min each step. The samples were then infiltrated with a 1:1 mixture of LR White resin—95% ethanol for 4 h, room temperature, and then twice with 100% LR White resin for 4–8 h. The samples were further cured in 100% LR White resin at 50°C for 48 h. The 90-nm-thick sections were mounted on 200 mesh Piloform-coated nickel grids. For immunostaining, grids were incubated 60 min in blocking solution containing 0.1% bovine serum albumin (BSA) and 0.1% Tween in PBS, pH 7.4. Immediately after blocking, sections were incubated overnight at room temperature with or without (control) affinity-purified FGFR1 antibody in PBS. The same polyclonal C-term FGFR1 Ab was used as for the immunofluorescent staining (see above). After washing three times with PBS, grids were incubated for 2 h with colloidal gold-conjugated (5 or 10 μm) goat anti-rabbit IgG (2 μg/ml in PBS, pH 7.4, and 0.5% fetal calf serum). Sections were washed three times in PBS, fixed for 2 min with 0.1% glutaraldehyde, and washed two times for 5 min in 5 mM glycine in PBS and in distilled H_2O (3 times). The sections were subsequently stained with saturated uranyl acetate in H_2O for 10 min and washed several times with H_2O. The sections were observed in a Joel 100 CX transmission electron microscope at 80 kV. Control samples processed without the first antibody showed no staining.

RESULTS

Scatchard Analysis of ^{125}I-FGF-2 Binding to BAMC

To ascertain whether the nucleus contains functional FGFR capable of interacting with FGF-2, we examined the binding of ^{125}I-FGF-2 to subcellular fractions obtained from BAMC (Table 1). The cell surface binding data, analyzed by the method of Scatchard (Scatchard, 1949), were consistent with a two-component binding curve, indicating the presence of both low- and high-affinity ^{125}I-FGF-2 binding sites. Low- and high-affinity FGF-2 binding sites also were detected in the cytoplasm, whereas only high-affinity sites (78 pm) were found in the nuclear fraction. On the cell surface, the low-affinity sites were 17-fold more abundant than the high-affinity sites (Table 1). In the cytoplasm, this difference was 2.4-fold. The number of high-affinity sites in the nucleus was 15-fold higher than in the cytoplasm and 12-fold higher than on the cell surface. In all cases, specific binding was eliminated by a 100-fold excess of unlabeled FGF-2.

Table 1. Affinity and number of ^{125}I-FGF-2 binding sites on the surface and in the cytoplasmic and nuclear fractions of BAMC

	Low affinity		High affinity		Low High
	Kd (nM)	No./cell	Kd (pM)	No./cell	No./cell
cell surface	6	20,000	1.5	1200	17
cytoplasmic fraction	1.5	2300	86	900	2.6
nuclear fraction		ND	78	14,500	—

Cells were fractionated, and specific ^{125}I-FGF-2 binding was determined as described in materials and methods. Scatchard analysis revealed low- and high-affinity ^{125}I-FGF-2 binding sites on the cell surface and in the cytoplasm. The r values for the low- and high-affinity surface receptors were 0.89 and 0.93 and for the cytoplasmic receptors 0.92 and 0.97, respectively. The nuclear fraction contains only the high-affinity sites; r = 0.91; ND = not detected.

FGFR1 Is the Major High-Affinity FGF Receptor on BAMC

To identify the types of high-affinity FGFR expressed in BAMC, cells were incubated with ^{125}I-FGF-2 and cross-linked with DSS, and the ligand–receptor complexes were immunoprecipitated with antibodies to FGFR 1-4 or normal rabbit IgG (Figure 1). We detected only FGFR1 protein. The apparent molecular size of cross-linked FGFR1–FGF-2 complexes ranged from ~130 to 165 kDa.

Western Blot Analysis of FGFR1 in Subcellular Fractions

Western blot analysis with McAb6 directed against the extracellular domain of FGFR1 detected receptor bands of 103, 118, and 145 kDa in BAMC (Figure 2). To determine the subcellular localization of FGFR1, we fractionated BAMC by two different methods. In one fractionation protocol, BAMC were lysed with 0.6% NP-40 in hypotonic buffer, and nuclei were separated from the extranuclear material by centrifugation. Analysis of the isolated nuclei by phase-contrast microscopy showed little contamination with cytoplasmic membranes and organelles. The purity of the isolated nuclei was confirmed via biochemical assays of marker enzymes. The nuclear fraction contained <5% of the total cellular activity of 5′nucleotidase (plasma membrane marker) and <2% of total activity of acid phosphatase (lysosomal marker). The specific content of FGFR1 in the nuclei was approximately threefold higher than in the extranuclear fraction (Figure 2A). The second method (Boyle *et al.*, 1985; Stachowiak *et al.*, 1994, 1996) involved isotonic cell lysis and purification of the nuclei through a sucrose cushion and produced similar results (Figure 2B). The purified nuclei contained ~10% of the total cellular activity of 5′nucleotidase and 2% of the total activity of acid phosphatase.

To determine whether nuclear receptors detected by Western blot analysis represent full-length FGFR1, the

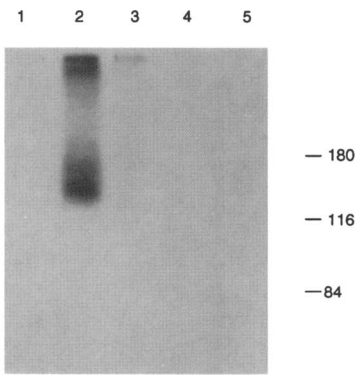

Figure 1. Cross-linking of ^{125}I-FGF-2 to BAMC. ^{125}I-FGF-2 was bound to BAMC at 4°C. The ligand was cross-linked to receptor with DSS, and the ligand–receptor complexes were solubilized with 1% Triton X-100 and immunoprecipitated with antibodies specific to the C-terminal domains of FGFR1 (lane 2), FGFR2 (lane 3), FGFR3 (lane 4), or FGFR4 (lane 5). In lane 1, a normal rabbit IgG was used. Migration of molecular weight standards is indicated at right.

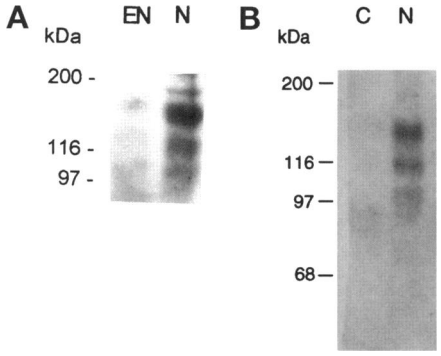

Figure 2. Western analysis of FGFR1 in subcellular fractions of BAMC. (A) BAMC were lysed with 0.6% NP-40 in hypotonic HEPES buffer, and nuclei (N) were separated from the extranuclear material (EN) by centrifugation as in Schreiber *et al.* (1989). (B) BAMC were lysed with isotonic nuclear buffer containing 0.1% digitonin. Nuclei (N) and the cytoplasmic fraction (C) were isolated according to Boyle *et al.* (1985). Fifty micrograms of proteins were used in each lane. Blots were probed with a monoclonal (McAb6) FGFR1 antibody. Numbers indicate molecular weight standards.

nuclear extracts were immunoprecipitated with antibodies against the intracellular C-terminal domain of FGFR1 (C-term FGFR1 Ab or commercial FGFR1 antibody; Santa Cruz Biotechnology) or with control IgG, and the immunoprecipitates were separated on SDS-polyacrylamide gels along with the whole-nuclear extracts and subjected to Western analysis with McAb6 antibody (Figure 3). As with the total nuclear extracts (Figure 3, lanes 1 and 4), McAb6 recognized the 103-, 118-, and 145-kDa FGFR1 isoforms immunoprecipitated with the C-term FGFR1 antibodies (lanes 3 and 6).

Microscopic Analysis of FGFR1 Localization in BAMC

To further confirm the nuclear localization of FGFR1, we used immunocytochemistry with confocal and electron microscopy. The subcellular distribution of FGFR1 immunoreactivity was first analyzed in BAMC stained with the C-term FGFR1 Ab by using two-dimensional projections of a series of confocal images (Figure 4, A–C). Some BAMC showed a weak cytoplasmic FGFR1 immunofluorescence (FGFR1-IF) and cell perimeter staining (Figure 4A). This pattern of immunoreactivity may be due to cytoplasmic and plasma membrane-associated FGFR1. Most cells showed a distinct nuclear presence of FGFR1-IF. The extent of nuclear labeling varied; some cells contained a few spots, whereas others showed labeling of the entire nucleus. The same pattern of staining was observed when immune complexes were visualized with peroxidase and diaminobenzidine via the technique described in Stachowiak *et al.* (1994; and our unpublished observations). Omitting the C-term FGFR1 Ab (Figure 4A) or replacing it with preimmune serum abolished both the nuclear and cytoplasmic staining (our unpublished observations). The specific nuclear immunofluorescence also was eliminated when the C-term FGFR1 Ab was preincubated with an excess of its cognate peptide (Figure 4B). However, under these conditions the cells showed some residual cytoplasmic immunofluorescence, which may reflect incomplete neutralization of the antibody and/or a low level of nonspecific binding of the primary antibody. Using the same staining protocol as for FGFR1, we detected the non-nuclear enzyme tyrosine hydroxylase exclusively in the cytoplasm (our unpublished results).

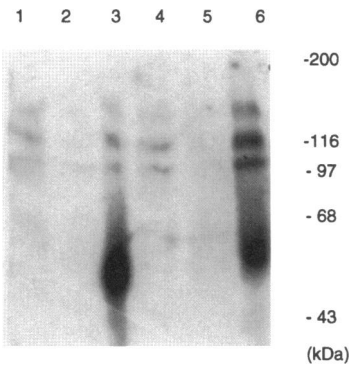

Figure 3. Nuclear FGFR1 contains both the C-terminal (intracellular) and N-terminal (extracellular, ligand-binding) domains. Nuclear extracts were incubated overnight with the C-term FGFR1 Ab (10 μg; lanes 2 and 3) or with a commercial C-terminal FGFR1 antibody (1 μg; lanes 5 and 6; Santa Cruz Biotechnology). The immunoprecipitates were collected on protein A-Sepharose and subjected to Western blot analysis with the monoclonal antibody against the extracellular domain of FGFR1 (McAb6). Lanes 1 and 4, nuclear extract before immunoprecipitation; lanes 2 and 5, supernatant remaining after FGFR1 immunoprecipitation; lanes 3 and 6, immunoprecipitated FGFR1.

The observed pattern of nuclear immunofluorescence could be due to either nuclear membrane or intranuclear staining. To distinguish between these localizations, we analyzed a series of consecutive 1-μm confocal laser sections through BAMC stained with the C-term FGFR1 antibodies. The pattern in these sections shows that FGFR1-IF is present within the nuclear interior (Figure 4D). The same pattern of staining was obtained by using the monoclonal antibody (McAb6) against the extracellular domain of FGFR1 (Figure 4E).

To further ascertain the intranuclear localization of FGFR1, we stained ultrathin sections of cultured BAMC with the C-term FGFR1 Ab and secondary gold-conjugated IgG and analyzed them under the electron microscope. Labeling with the 10-nm immunogold particles was observed in sections treated with the C-term FGFR1 Ab but not in sections in which the primary antibody was omitted (our unpublished observations). Figure 5 shows the distribution of FGFR1-immunoreactivity (FGFR1-IR) in different areas within BAMC. FGFR1-IR was detected in the cytoplasm in areas containing dense core secretory vesicles (Figure 5, A and B). The immunogold particles appeared in clusters, but relatively few were associated with the vesicle bodies. Only a few groups of particles were observed in the plasma membrane (Figure 5A). FGFR1 labeling also was concentrated in central areas of the cytoplasm close to the nucleus, traversing the nuclear membrane, and inside the nucleus (Figure 5, B and C). FGFR1 was concentrated only in a few regions of the nuclear envelope, suggesting that the receptor is transported at specific sites on the nuclear membrane. Within the nucleus, FGFR1-IR displayed a patchy distribution. This patchy distribution illustrates the low level of background staining and suggests that FGFR1 may bind to specialized regions of the nucleus.

Regulation of Nuclear Content of FGFR1

In BAMC, stimulation of adenylate cyclase results in the accumulation of FGF-2 in the nucleus. In contrast, stimulation of the protein kinase C signaling pathway leads to an accumulation of FGF-2 in the cytosol (Stachowiak *et al.*, 1994). To determine whether nuclear accumulation of FGFR1 is coregulated with FGF-2, BAMC were maintained in serum-free medium for 40–48 h and then treated with 5 uM forskolin or 0.1 uM PMA. Figure 6 shows the results of an experiment in which cells treated with forskolin or PMA were separated into cytoplasmic and nuclear fractions and subjected to Western analysis with the monoclonal FGFR1 antibody (McAb6). Similar results were obtained in three independent experiments. In nuclear extracts from the control cells, McAb6 detected bands of 103, 118, and 145 kDa. Only trace amounts of these bands were found in the cytoplasmic fraction. The nuclear content of FGFR1 showed little or no detectable changes in cells treated with forskolin for 30–60 min (Figure 6A). However, treatment with forskolin for 4 or 8 h produced increases in the intensity of all three FGFR1 bands in the nuclear fraction. Densitometric scanning of the autoradiograms showed that, after 8 h of forskolin treatment, the intensity of the 145- and 118-kDa nuclear FGFR1 bands increased three- to fivefold, whereas the intensity of the 103-kDa FGFR1 band increased three- to fourfold. These increases were sustained for at least 12 h of forskolin treatment and then declined after 24 h (Figure 6B). In contrast to forskolin, a 4-h treatment with PMA had no effect on nuclear FGFR1 levels (Figure 6A). Thus, the nuclear translocation of FGFR1 is affected by the stimulation of intracellular signaling pathways in a manner similar to that of FGF-2. Nuclear induction of the 103-kDa FGFR1 band by forskolin was also observed by using the polyclonal C-term FGFR1 Ab (Figure 6D). In Western blots, little or none of 145- and 118-kDa FGFR1 were detected by the C-term FGFR1 Ab. Incubation with the translational inhibitor cycloheximide (20 uM) prevented the forskolin-induced increase in nuclear FGFR1 content, suggesting that the increase might result from enhanced FGFR1 synthesis (our unpublished observations).

Cultured, stimulated BAMC do not release measurable amounts of FGF-2 (Stachowiak *et al.*, 1994). Therefore, it is unlikely that the nuclear accumulation of FGFR1 is due to the interaction of extracellular ligand with cell surface FGF receptors, followed by internalization of the receptor. Nevertheless, we examined whether exogenous FGF-2 can induce the nuclear accumulation of FGFR1. Figure 6, B and C, shows Western analyses of FGFR1 in nuclear and cytoplasmic fractions of BAMC incubated with 5×10^{-9} M recombinant bovine FGF-2. In contrast to the results obtained with forskolin, FGF-2 did not increase the amount of FGFR1 associated with the nuclei.

The induction of nuclear FGFR1 by forskolin was confirmed via immunofluorescent staining and confocal microscopy (Figure 7A). The majority of control cells maintained in serum-free medium for 48 h showed a weak FGFR1-IF within the cytoplasm and on the cell perimeter. A few cells showed weak nuclear staining. After a 15-min incubation with forskolin, bright spots of FGFR-IF were observed in the cytoplasm. Forty-five minutes later, cytoplasmic FGFR-IF had increased. At this time, the FGFR1-IF accumulated in the cytoplasm in the region surrounding the nucleus and in some cells also within the nucleus. After 4 h, the nuclear FGFR1-IF had increased markedly; the entire nucleus was filled with FGFR1-IF. In some cells, FGFR1-IF also increased in the cytoplasm and in the plasma membrane. Similar changes were observed in the subcellular distribution of FGF-2 after 4 h of forskolin treatment (Figure 7B). To determine whether the growth factor and its receptor are found in the same nuclei, BAMC were double stained for FGFR1 and FGF-2 and subjected to confocal microscopic analysis (Figure 7C). Control cells showed low levels of FGF-2-IF (illustrated in green) predominantly outside the nuclei, whereas little or no FGFR1-IF (shown as red) was detectable. After 1 h of forskolin treatment, some cells displayed an increase in nuclear FGF-2-IF, whereas others showed colocalization of FGF-2 and FGFR1 in the nucleus (illustrated in yellow). After 4 h of forskolin treatment, when the induction of nuclear FGFR1 is maximal (Figure 7A), all cells showed colocalization of FGF-2-IF and FGFR1-IF (Figure 7C). Analysis of a series of individual consecutive 1-μm confocal laser sections through control and forskolin-treated BAMC demonstrated that the forskolin-induced accumulation of FGFR1 occurred inside the nucleus.

Physiologically, an increase in the levels of cAMP in adrenal medullary cells is induced by trans-synaptic (Guidotti and Costa, 1974) or hormonal (Boarder *et al.*, 1988) stimulation. Most splanchnic nerve terminals innervating the adrenal medulla contain and release acetylcholine. To determine whether cholinergic stimulation affects the nuclear FGFR1 content, we incubated BAMC with 0.2 mM carbachol. This acetylcholine analogue stimulates both the nicotinic and muscarinic receptors. Carbachol produced an increase in nuclear FGFR1-IF similar to forskolin (Figure 8). In some cells, the increase in nuclear FGFR1-IF was detected within 1 h of treatment. The nuclear labeling reached a maximum at 4–8 h. After 24 h, FGFR1-IF declined to control levels in the majority of BAMC. Nuclear

FGFR1-IF also was enhanced in BAMC treated with the angiotensin II agonist, 0.1 uM sar^1-angiotensin II (Figure 8). Thus, stimulation of neurotransmitter (acetylcholine) or hormonal (angiotensin II) receptors or the direct stimulation of the cAMP signaling pathway with forskolin increases the nuclear content of FGFR1 in a manner similar to that of FGF-2 (Stachowiak *et al.*, 1994; A. Joy and M.K. Stachowiak, unpublished data).

Nuclear FGFR1 Binds FGF-2 and Has Kinase Activity

To ascertain that intracellular FGFR1 binds FGF-2, nuclear and cytoplasmic extracts were incubated with ^{125}I-FGF-2, cross-linked with DSS, and immunoprecipitated with the C-terminal FGFR1 antibody. FGFR1–^{125}I-FGF-2 complexes formed by using nuclear extracts in the presence of the cross-linking agent DSS are shown on Figure 9A.

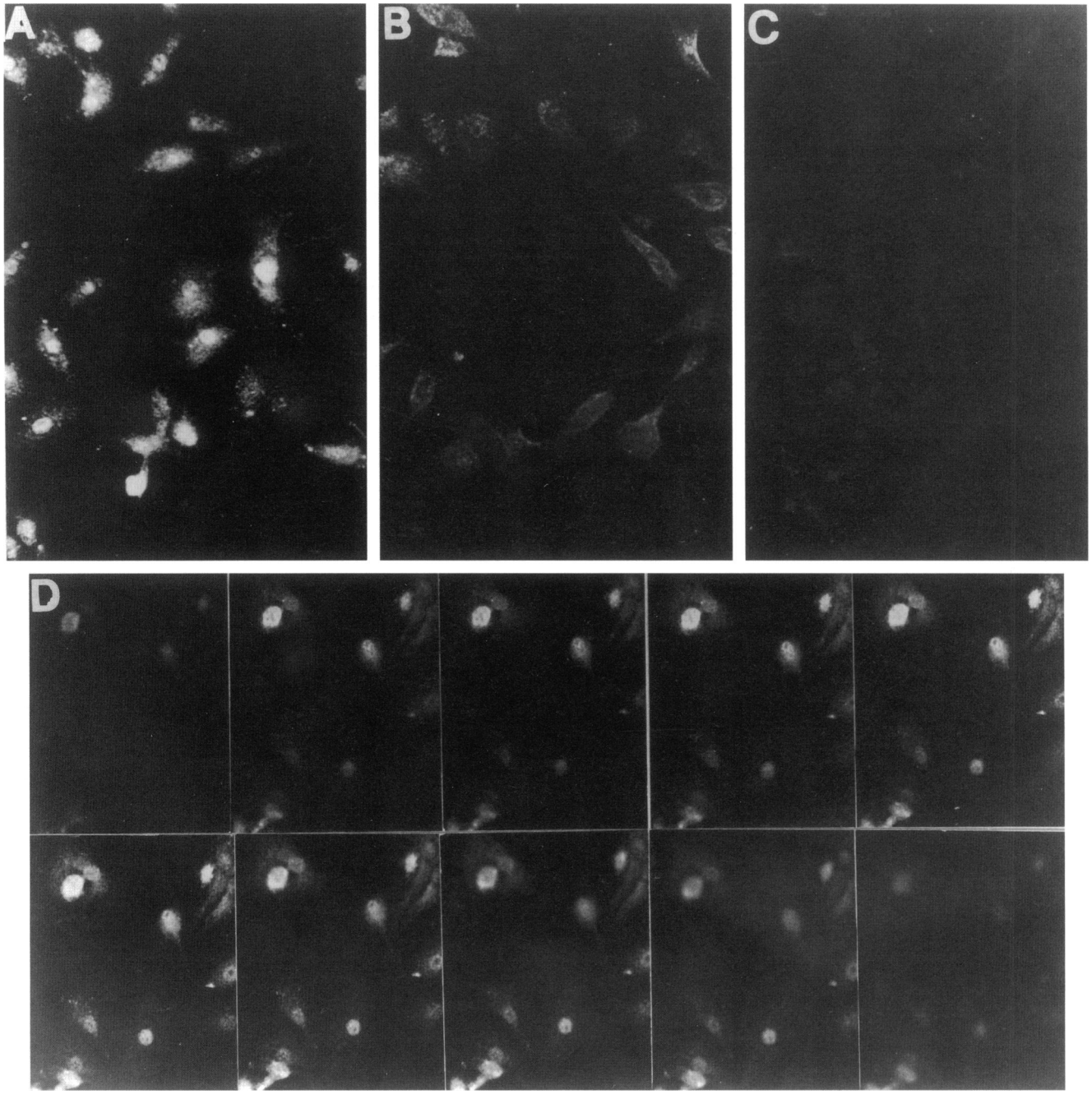

Figure 4.

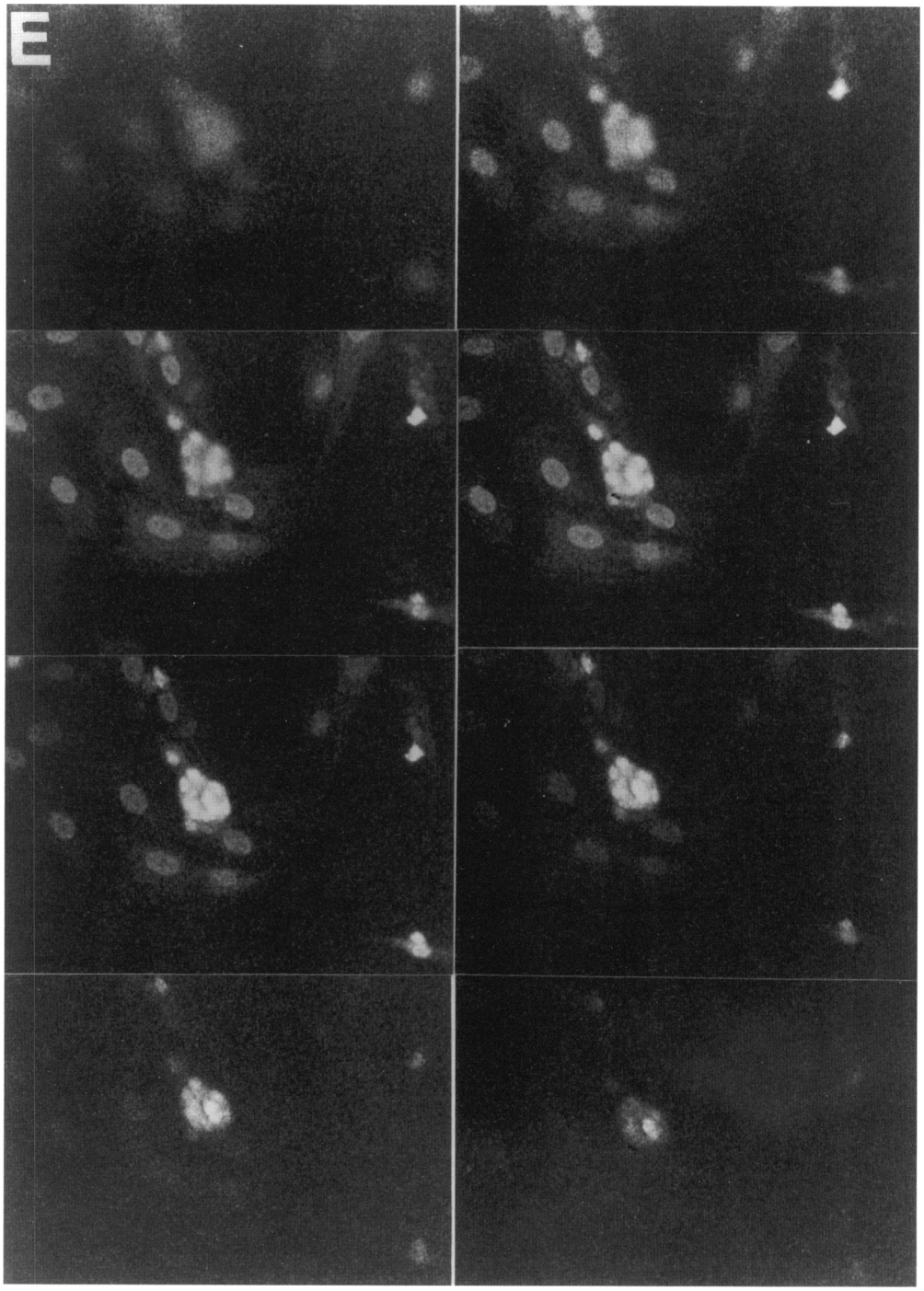

Figure 4 (cont). Confocal immunocytochemical localization of FGF receptor (FGFR1) in BAMC. BAMC were fixed, permeabilized with 1% Triton X-100, and incubated sequentially with the polyclonal C-term FGFR1 Ab and anti-rabbit CY^3-conjugated goat IgG (A–D) or the monoclonal FGFR1 Ab (MCAb6) and anti-mouse Cy^5-conjugated goat IgG (E). (A–C) Photographs represent stacked confocal laser sections taken 1 μm apart. No staining was observed when primary antibody was omitted (C). Preincubation of the C-term FGFR1 Ab (2 μg/ml) for 2 h at 4°C with the cognate peptide (20 μg/ml) abolished nuclear and most cytoplasmic FGFR1 immunofluorescence (B). (D) Individual confocal sections taken 5 μm (sections 1 and 2) or 1 μm (sections 2–10) apart through BAMC stained with the C-term FGFR1 Ab. (E) Individual consecutive confocal sections taken 1 μm apart through BAMC stained with McAB6. No fluorescence was detected when McAb6 antibody was omitted (Stachowiak, unpublished observation). Sections illustrate the intranuclear localization of the receptor.

To determine whether nuclear FGFR1 retains tyrosine kinase activity, nuclei were solubilized by sonication in a detergent-containing buffer, FGFR1 was immunoprecipitated with an antibody directed against the C-terminal domain of FGFR1, and the immunoprecipitate was assayed for autophosphorylation. As shown in Figure 9B, three high-molecular-weight phosphorylated bands, similar in size to the 145-, 118-, and 103-kDa FGFR1 bands detected by immunoblotting (Figures 2 and 3), are seen in receptor immunoprecipitates prepared with nuclei isolated from BAMC. In addition, a few unidentified higher-molecular-weight coprecipitating products became specifically phosphory-

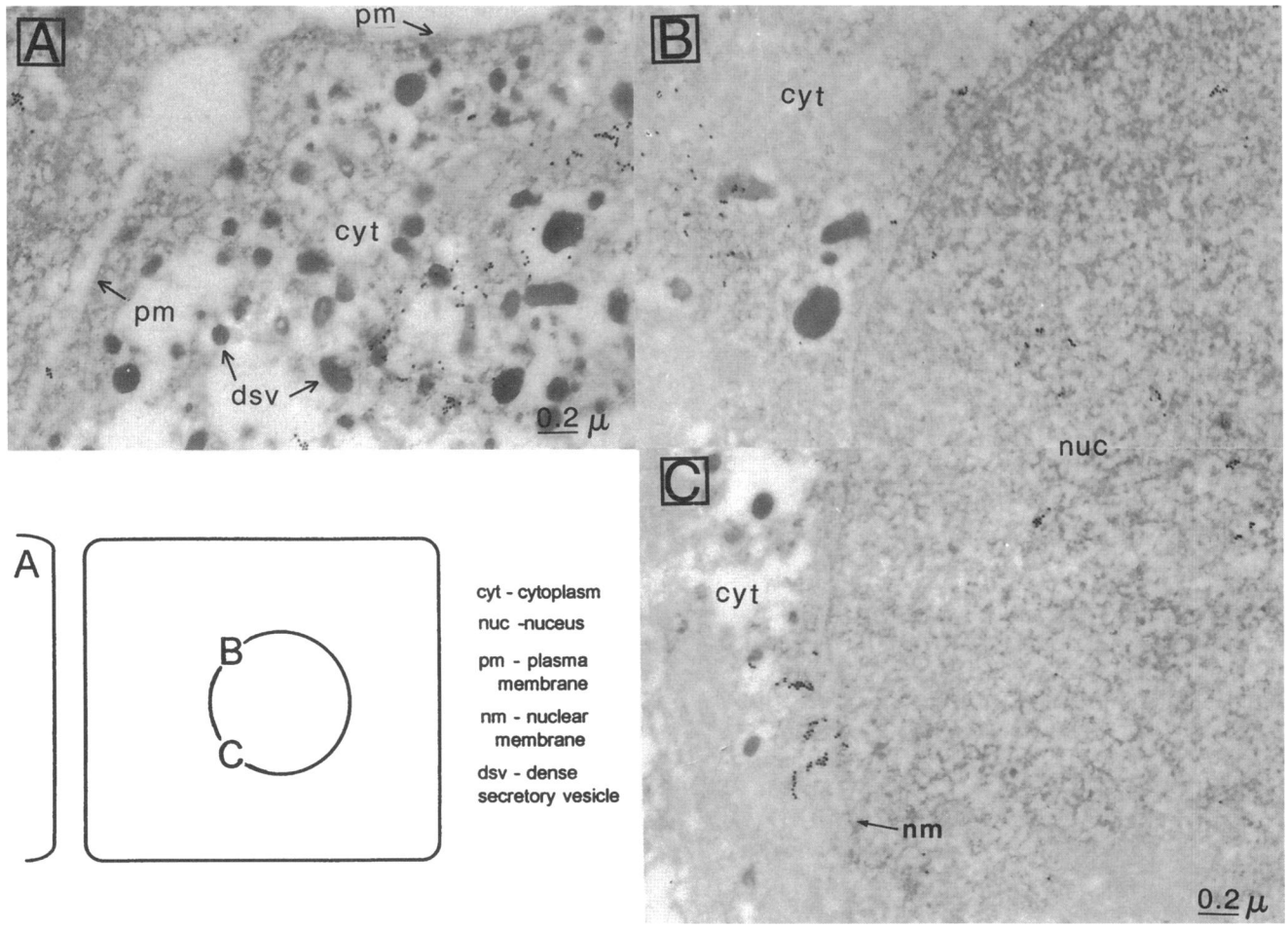

Figure 5. Electron microscopic analysis of FGFR1 distribution in BAMC. Thin sections of resin-embedded whole cells were immunostained with the affinity-purified polyclonal C-term FGFR1 Ab (same as in Figures 3, 4, 6D, 7, and 8) and immunogold-conjugated anti-rabbit IgG. The drawing shows cell areas from which photographs were taken.

lated. Treatment of the cells with forskolin increased the intensity of the phosphorylated bands (Figure 9B).

These results suggested that nuclear FGFR1 might bring about a general increase in FGF-2–inducible tyrosine kinase activity in the nucleus. To test this idea, nuclei from control and forskolin-treated cells were assayed for tyrosine kinase activity in the absence or presence of added FGF-2 (100 ng/ml) by using poly glu/tyr (4:1) as an exogenous substrate. The FGF-2–induced phosphorylation of the substrate was increased from 23.4 (cpm/μg protein/pmol substrate/20 min) in the nuclear extracts from control BAMC to 92.2 (cpm/μg protein/pmol substrate/20 min) in nuclei from cells incubated with forskolin for 4 h.

Subnuclear Localization of FGFR1

The targeting of functional FGFR1 and FGF-2 to the nucleus of BAMC suggests that FGFR1 and its ligand may use an intracrine mechanism to mediate functional responses to neurotransmitter and hormone stimulation. To begin an analysis of the nuclear function of FGFR1, we investigated its subnuclear compartmentalization. We sequentially fractionated nuclei to give soluble nucleoplasmic proteins, chromatin-associated proteins, and the nuclear matrix–lamina complex and then performed Western analysis for FGFR1 in each fraction by using the monoclonal FGFR1 antibody (McAb6; Figure 10). Within the nucleus, ~60% of FGFR1 is associated with the nuclear matrix–lamina complex and 40% with the nucleoplasmic fraction. No FGFR1 was detected in the chromatin fraction. In addition, there are differences in the distribution of the different molecular weight forms of FGFR1 detected with McAb6. The nuclear matrix contains equal amounts of the 145- and 118-kDa FGFR1 proteins and only

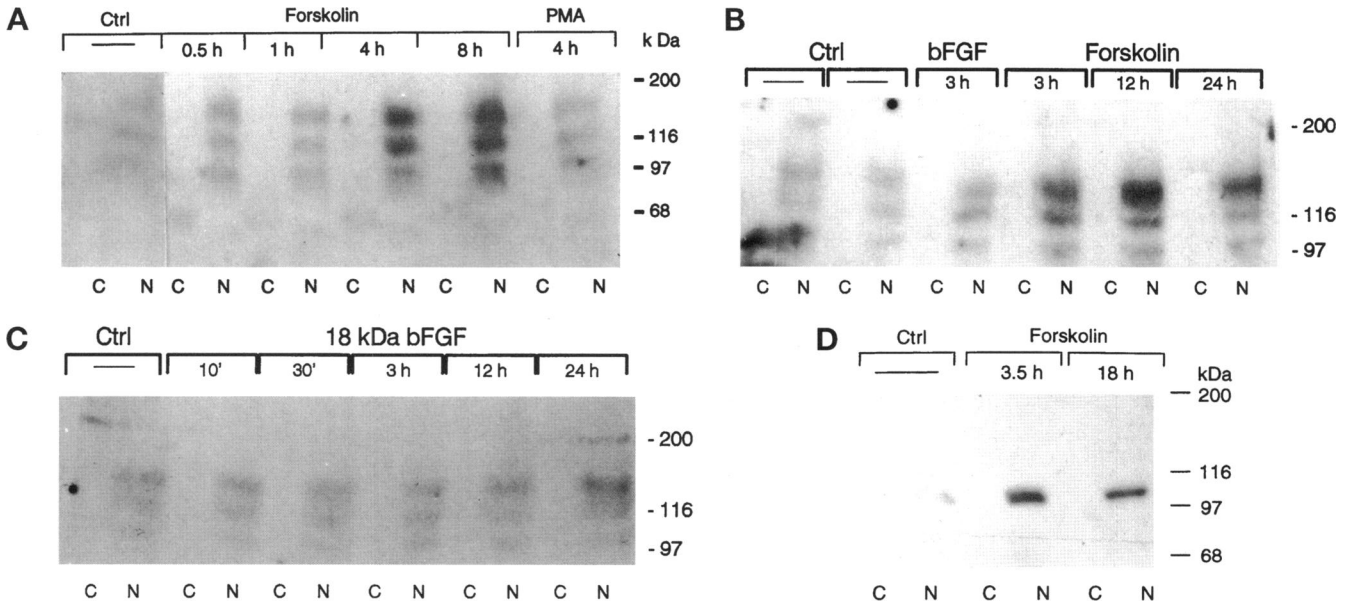

Figure 6. Forskolin increases the amount of nuclear-associated FGFR1. BAMC were cultured in serum-free medium and treated with 5 uM forskolin (A, B, and D), 0.1 uM PMA (A), or 5 nM FGF-2 (bFGF; B and C) for the indicated periods of time. Cytoplasmic and nuclear fractions were isolated as described in MATERIALS AND METHODS and were subjected to Western analysis with the monoclonal FGFR1 antibody (McAb6; A–C) or with the polyclonal C-term FGFR1 Ab (D). Migration of molecular weight protein standards is indicated to the right of the autoradiograms.

trace amounts of the 103-kDa protein. In the nucleoplasm, the 145-kDa band is the most abundant FGFR1, followed by the 103- and the 118-kDa band. Treatment with forskolin increased the FGFR1 content in the nucleoplasmic fraction.

The nuclear matrix–lamina complex consists of a lamina and a system of intranuclear fibers (He *et al.*, 1990). In the present study we used immunoelectron microscopy to distinguish between peripheral and interior nuclear matrix localizations of FGFR1. Nuclear matrix was prepared by sequentially extracting adherent BAMC on slides to remove cytoplasmic material, nucleoplasm, and chromatin-associated proteins plus DNA. The nuclear matrix prepared by this method was subjected to conventional embedded section microscopic analysis with immunogold labeling for FGFR1. The general appearance of the matrix is shown in Figure 11A. Although the three-dimensional ultrastructure of the matrix cannot be visualized by using resin-embedded slices, it is still possible to determine the general location of nuclear matrix-associated FGFR1. In a high-magnification view, numerous clusters of 5-nm gold beads are seen decorating the interior of the nuclear matrix (Figure 11B). This patchy distribution suggests that FGFR1 may bind to specific matrix components and play a role within specialized regions of the nuclear matrix.

DISCUSSION

Functional FGF Receptor Is Localized in the Nucleus

In the nervous system, the execution of genetic programs for cell growth, proliferation, and differentiation are governed by the sequential expression of growth factors and their receptors (Yamamori, 1990). Peptide growth factors are generally thought to produce their biological effects by interacting with cell surface receptors. Evidence is mounting, however, that growth factors have an important, additional signaling role directly within the nucleus (reviewed, Burwen and Jones, 1987; Jans, 1994). The studies reported here demonstrate the nuclear localization of functional FGF-2 receptors in BAMC. Initially, we showed the presence of the FGF-2 binding sites in the nuclear fraction. Nuclear sites bind FGF-2 with a K_d of 78 pm. This value lies within the range for high-affinity FGFR found in variety of cell types (Moscatelli, 1987; Allen and Maher, 1993). The K_d of the high-affinity nuclear and cytoplasmic FGF-2 binding sites is somewhat higher than the K_d of the cell surface sites, which could be a reflection of either different receptor conformations or protein–protein interactions. The number of high-affinity FGF-2 binding sites in the nuclei is several-fold higher than on the cell surface or in the cytoplasmic fraction.

Using Western blot analysis as well cross-linking to [^{125}I]-FGF-2 and immunoprecipitation, we have iden-

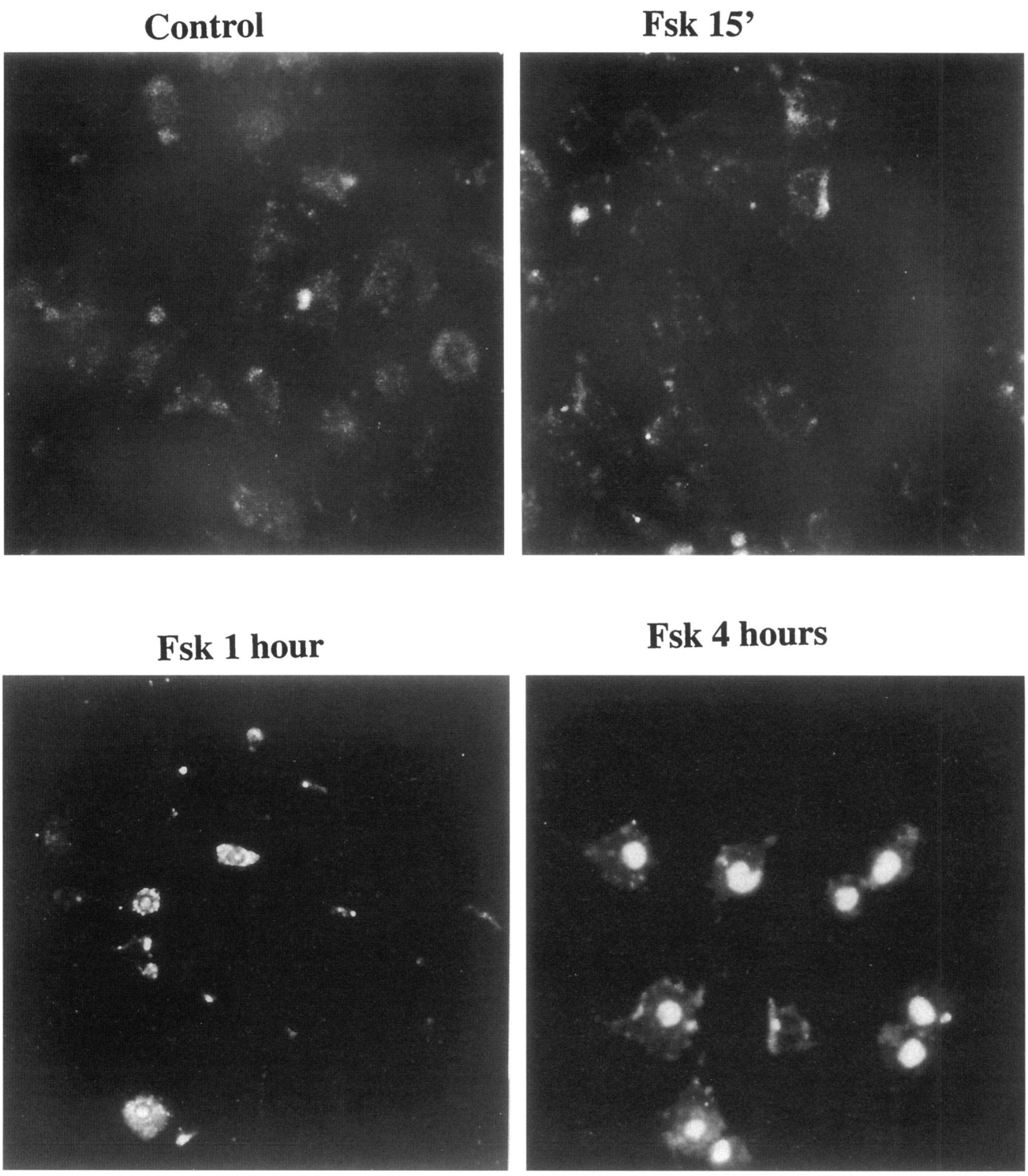

Figure 7.

tified the nuclear FGF-2 receptors as FGFR1. Indeed, in BAMC the majority of the total cellular FGFR1 is associated with the nuclear fraction. The presence of FGFR1 in isolated nuclei is unlikely to be an artifact of the isolation techniques. Microscopic examination of isolated nuclei showed little extranuclear material.

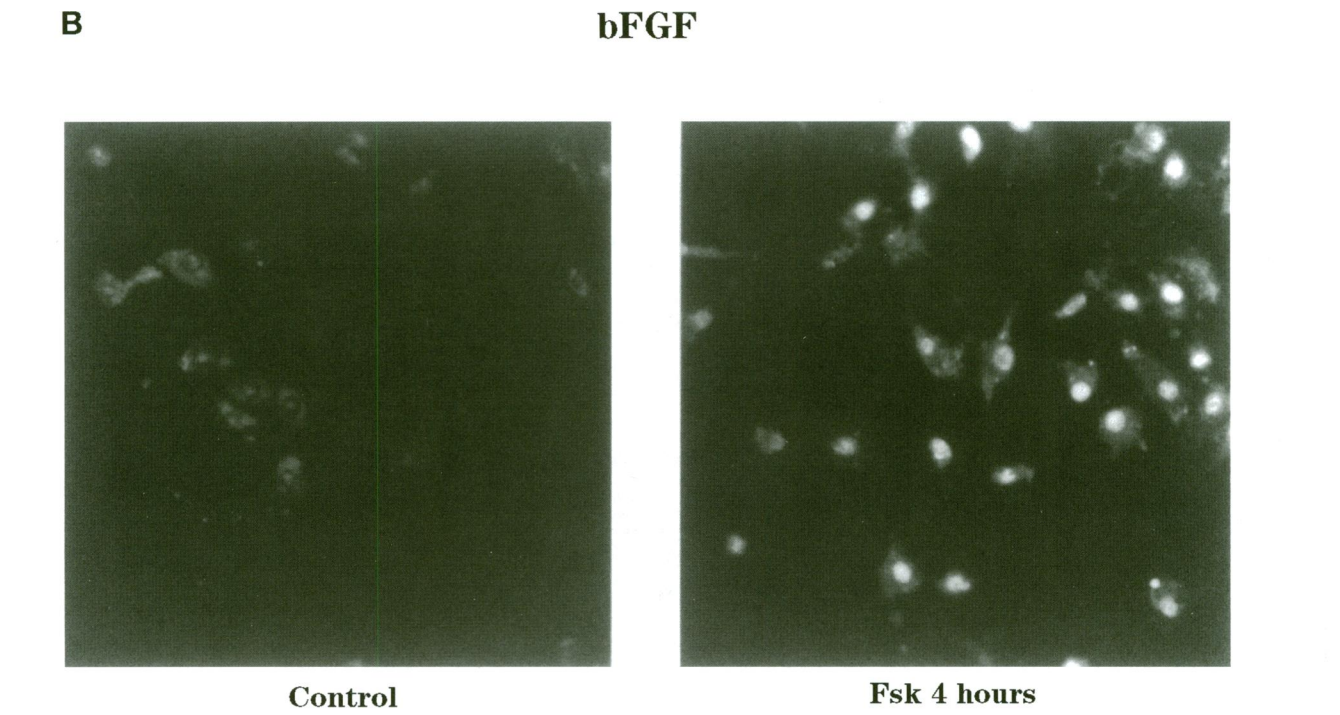

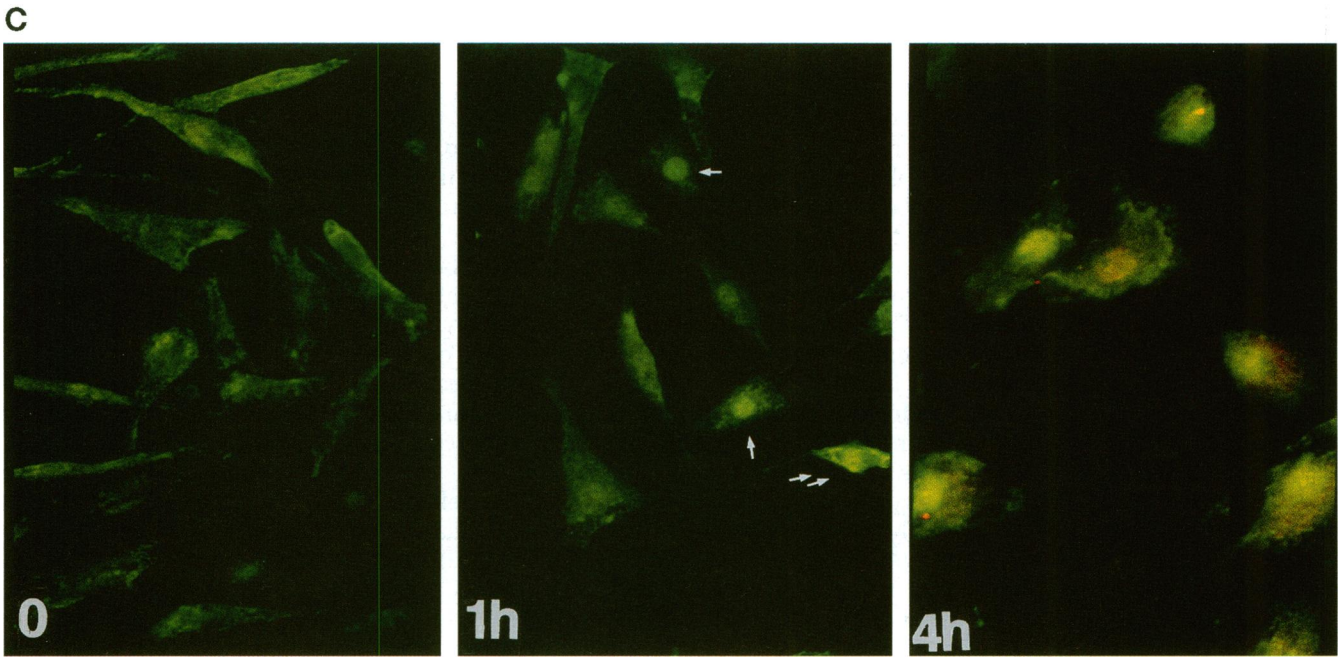

Figure 7 (cont). Effect of forskolin on the subcellular distribution of FGFR1 and FGF-2 in BAMC-immunofluorescent confocal analysis. Cultured BAMC were maintained in a serum-free medium for 40 h and then treated with 5 uM forskolin for the indicated period of time. Figure shows two-dimensional projections of stacked optical confocal sections taken 1 μm apart. (A) FGFR1 cells were incubated with the polyclonal C-term FGFR1 Ab and stained with Cy^3-goat anti-rabbit IgG. (B) FGF-2 cells were incubated with a monoclonal FGF-2 antibody and stained with Cy^5-goat anti-mouse IgG. (C) Colocalization of FGFR1-IF and FGF-2-IF. BAMC were incubated with the C-term FGFR1 Ab and an FGF-2 Ab, and the immune complexes were stained with Cy^3-goat anti-rabbit IgG (FGFR1) and Cy^5-goat anti-mouse IgG (FGF-2). Colors: Green illustrates FGF-2; red, FGFR1; yellow, colocalization of the FGF-2 and FGFR1 immunofluorescence. At 1 h of forskolin treatment, some cells displayed only FGF-2 (arrow) and some both the FGF-2 and FGFR-1 immunofluorescence (double arrow). At 4 h all cells showed colocalization of FGF-2 and FGFR1 in the nuclei.

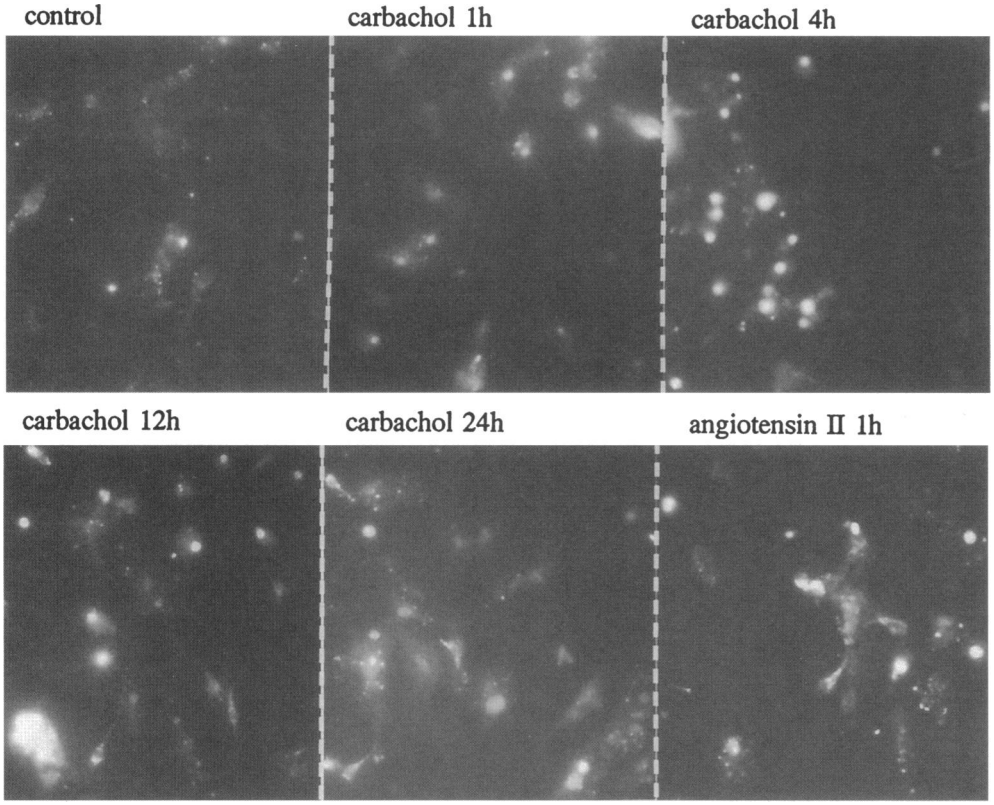

Figure 8. Effects of carbachol and angiotensin II on the subcellular distribution of FGFR1-immunofluorescence (FGFR1-IF) in BAMC. Cells were preincubated in serum-free medium for 48 h before treatment with 0.2 mM carbachol or 0.1 uM sar[1]-angiotensin II for the indicated period of time. BAMC were permeabilized with 1% Triton X-100 and incubated sequentially with the polyclonal C-term FGFR1 Ab and anti-rabbit IgG conjugated with rhodamine, as described in MATERIALS AND METHODS.

Also, analysis of marker enzymes indicates that the contamination of the nuclei with plasma membrane and lysosomal proteins is minimal. Low-affinity FGF-2 binding sites, which are present on the cell surface in far greater numbers than the high-affinity receptors, are not detected in the nuclear fraction. In further support for a specific nuclear localization of FGFR1, more than one-half of the total nuclear FGFR1 protein is associated with the 2-M NaCl insoluble nuclear matrix, although the protocol used for the isolation of the nuclear matrix removes nuclear membranes that may be contaminated by fragments of the endoplasmic reticulum. These findings suggest that nuclear FGFR1 is tightly associated with the nuclear matrix and that contamination of nuclei with loosely bound plasma or intracellular membrane proteins may be excluded. Localization of FGFR1 in the nuclear interior was confirmed by immunocytochemistry with well-characterized FGFR1-specific antibodies. The specificity of FGFR1 immunostaining was clearly demonstrated by a variety of controls as summarized in MATERIALS AND METHODS. Laser confocal microscopy demonstrated that specific FGFR1 immunofluorescence in BAMC is present predominantly within the nucleus, with little cytoplasmic or plasma membrane localization. Analysis of a series of confocal laser sections through the nucleus demonstrated that FGFR1 immunofluorescence is localized within the nucleus rather than associated with the nuclear surface. These results were confirmed by immunoelectron microscopy, which demonstrated the presence of FGFR1 protein both traversing the nuclear membrane and inside the nucleus.

We used several different antibodies to detect FGFR1 in the nuclei of BAMC. The same nuclear FGFR1 was detected with two different C-term FGFR1 antibodies (Santa Cruz Biotechnology; Hanneken *et al.*, 1995) that recognize the C-terminal domain of full-length FGFR1 and with a monoclonal antibody (McAb6; Hanneken *et al.*, 1995) directed against the extracellular, ligand-binding domain of FGFR1. This suggests that full-length functional FGFR1 are present in the nucleus. Consistent with these results, we show that nuclear FGFR1 binds FGF-2 and undergoes autophosphorylation. Thus, nuclear FGFR1 could serve as an effector kinase for nuclear FGF-2. The nuclear localization of FGFR1 is not unique to BAMC. We recently demonstrated that the nuclei of human glial cells also contain FGFR1 (Stachowiak *et al.*, 1996). Nuclear association has been reported for insulin (Podlecki *et al.*, 1987), epidermal growth factor (Rakowicz-Szulczynska *et al.*, 1989; Jiang and Schindler, 1990), and growth hormone (Lobie *et al.*, 1994) receptors and is well documented for steroid receptors

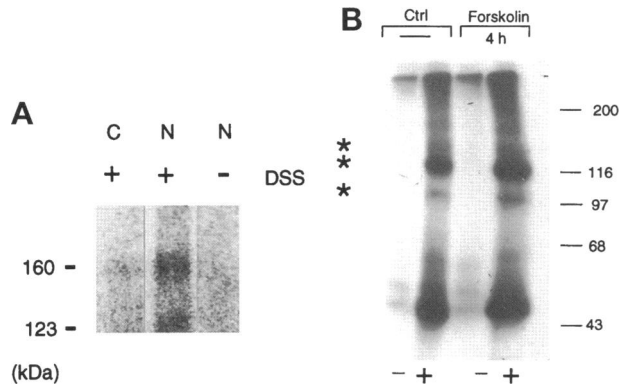

Figure 9. Binding of FGF-2 (A) and kinase activity (B) of nuclear FGFR1. (A) ^{125}I-FGF-2 was bound to nuclear or cytoplasmic fractions of BAMC and cross-linked with DSS. The nuclear (N) and cytoplasmic (C) complexes were immunoprecipitated with a C-terminal FGFR1 antibody (−, no DSS used; +, 0.15 mM DSS). Molecular weights of standards are indicated at left. (B) Kinase activity of nuclear FGFR1 in control and forskolin-treated cells. Immunoprecipitates were prepared from nuclear extracts of BAMC with 1 μg of an antibody directed against the C-terminal domain of FGFR1 (+) or control IgG (−), as described in MATERIALS AND METHODS. Immunoprecipitates were phosphorylated in vitro with gamma-^{32}P-ATP and resolved on SDS-7.5% polyacrylamide gels. Molecular weights (in kDa) are indicated at right. Bands marked with asterisks (~145, 118, and 103 kDa) indicate phosphorylated FGFR1. Only low-molecular-weight phosphorylated bands are seen in control immunoprecipitates that use normal rabbit IgG. The strong band at 55 kDa is IgG heavy chain.

(Beato, 1989). To the best of our knowledge, the results reported here are the first demonstration that the nuclear translocation of growth factor receptors is regulated by neurotransmitters, hormones, and their signaling pathways.

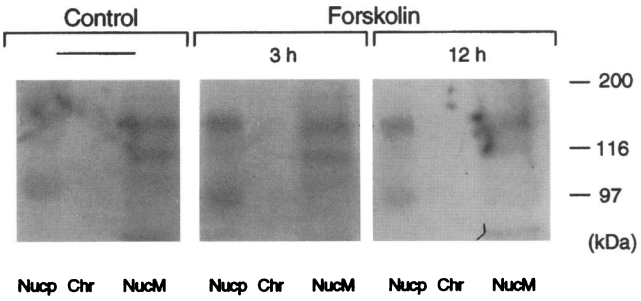

Figure 10. Western analysis of FGFR1 distribution in subnuclear fractions. The same number of nuclei (0.5–1.0 × 10^6) isolated from control and forskolin-treated cells was subjected to biochemical fractionation. Total nucleoplasm (Nucp) and chromatin (Chr) fractions were concentrated with WGA. The nuclear matrix (NucM) pellet was dissolved directly in 2.5× SDS-sample buffer. Proteins were electrophoresed on polyacrylamide gels, transferred to nitrocellulose membrane, and probed with a monoclonal FGFR1 antibody (McAb6) and ^{125}I-protein A. Autoradiograms were exposed for 1 d. Molecular weights are indicated at right.

How Is FGFR1 Translocated to the Nucleus?

The association of FGFR1 with the nucleus and its regulation by the cAMP pathway implies that a specific nuclear transport mechanism must exist for FGFR1. A macromolecule of the size of nuclear FGFR1 (103–145 kDa) would require active transport through the nuclear pore complex. Electron microscopy indicates that translocation of FGFR1 across the nuclear membrane is limited to a few regions of the nuclear envelope. Some of these regions were less electron dense, as is typical of nuclear pores (our unpublished results). The association of transported protein with the nuclear pore complex requires that it contain a nuclear localization signal (NLS; reviewed, Silver, 1991). Careful analysis shows no obvious NLS sequence in FGFR1. However, post-translational modifications of amino acids, such as arginine methylation, may generate an efficient NLS (reviewed, LaCasse and Lefebvre, 1995). Alternatively, proteins without NLS can be transported to the nucleus by binding to a protein that contains an NLS (Silver, 1991). In the case of FGFR1, the NLS could be provided by its ligands FGF-1 or FGF-2 (Imamura *et al.*, 1990; Bugler *et al.*, 1991; Lin *et al.*, 1996). Indeed, recent evidence suggests that the NLS of FGF-1 plays an important role in the mitogenic pathway initiated by this growth factor (Lin *et al.*, 1996). In BAMC FGF-2 translocates to the nucleus under the same conditions as FGFR1, and the time course of their translocation is similar. They both accumulate within the same nuclear compartments (Stachowiak *et al.*, 1994; A. Joy and M.K. Stachowiak, unpublished data). It remains to be determined whether nuclear translocation of FGFR1 requires ligand.

Cell membrane receptors for peptide growth factors internalize once they bind ligand, allowing the entry of actively transducing receptors into the cytoplasm (reviewed, Hopkins, 1994). Whether FGFR1 translocates into the nucleus with or without previous insertion into the plasma membrane is unknown. The size of the 103-kDa form of FGFR1 is similar to the largest FGFR1-1 isoform predicted from cDNA analysis (~96 kDa; Dionne *et al.*, 1990; Hou *et al.*, 1991), but it is smaller than the fully glycosylated receptor (~150 kDa; Xu *et al.*, 1992). We found that incubation of nuclear extracts with *N*-glycanase increases the electrophoretic mobility of the 145- and 118-kDa FGFR1 forms but has a little or no effect on the 103-kDa FGFR1 form (P.A. Maher and M.K. Stachowiak, unpublished results). Thus, the 103-kDa protein is a non- or hypoglycosylated form of FGFR1, whereas the 118- and 145-kDa proteins may represent hyperglycosylated receptor. Although the C-term FGFR1 Ab immunoprecipitated all three forms of FGFR1, in Western immunoblot assays the C-term FGFR1 Ab detected predominantly the 103-kDa FGFR1. This result is con-

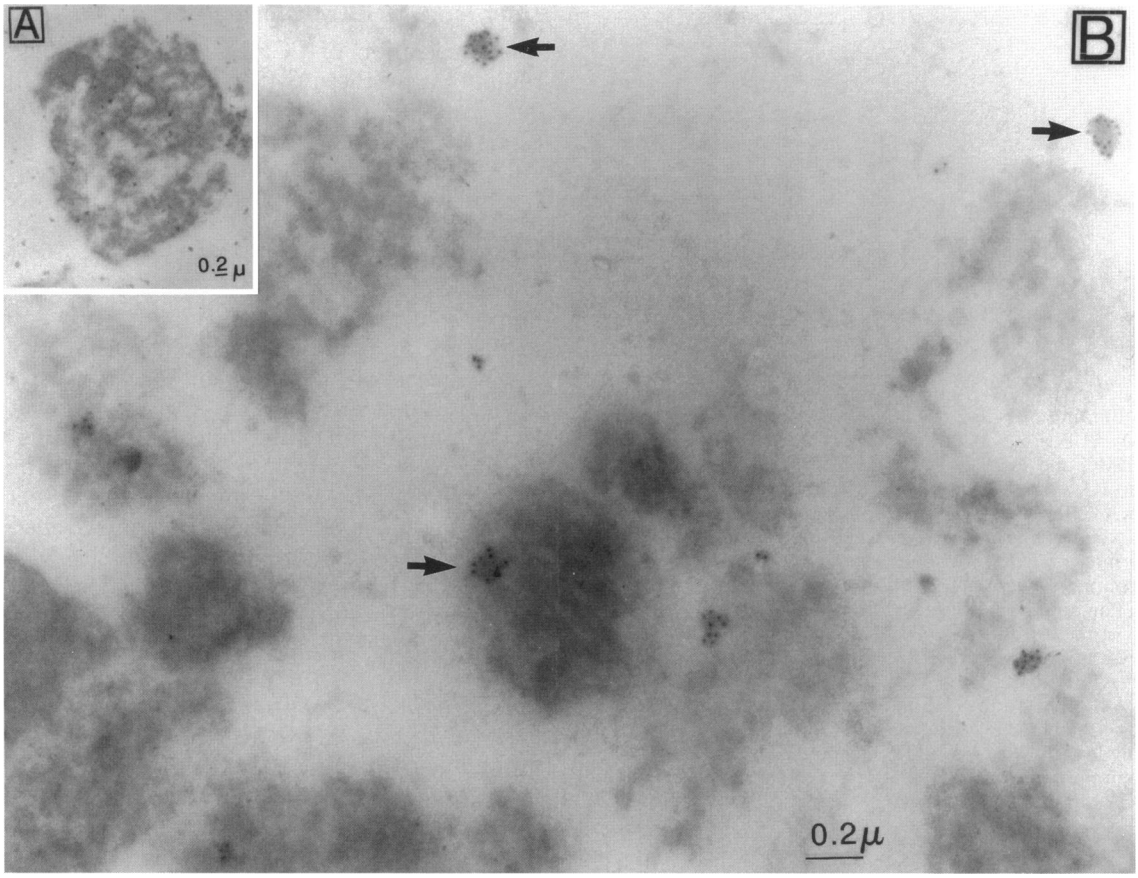

Figure 11. Immunoelectron microscopy of nuclear matrix associated FGFR1. (A) View of nuclear matrix. (B) Patchy distribution of FGFR1 immunoreactivity inside the nuclear matrix (examples marked with arrows).

sistent with the inefficient detection of hyperglycosylated FGFR1 by the C-term FGFR1 Ab (P. Maher, unpublished observation). The hypoglycosylated FGFR1 may still represent a functional receptor, because nonglycosylated FGFR1 can bind FGF-2 (Bergonzoni *et al.*, 1992). The appearance of glycosylated FGFR1 in the nucleus suggests that the receptor is processed through the Golgi apparatus before its nuclear translocation or is derived from plasma membrane.

The perinuclear accumulation of FGFR1 (Prudovsky *et al.*, 1994) was induced by exogenous FGF-1 and required a long-term (12 h) treatment of cells with ligand. In contrast, the intracellular accumulation of FGFR1 in BAMC was not affected by exogenous FGF-2 but was increased upon stimulation of cholinergic or angiotensin II receptors or by direct activation of adenylate cyclase with forskolin. These stimuli also increased the synthesis and cellular content of FGF-2 (Stachowiak *et al.*, 1994). However, because no FGF-2 was detected outside the BAMC, it is unlikely that these stimuli caused an increased interaction of cell surface FGFR1 with FGF-2. Nevertheless, it is possible that other members of the FGF family are made by BAMC and that the synthesis and release of these growth factors could be increased by neurotransmitter or hormonal stimulation. The nuclear accumulation of FGFR1 in BAMC occurs within 4 h of cell stimulation and is preceded by an increase in cytoplasmic FGFR1-IF without an apparent previous accumulation in the plasma membrane. Nuclear accumulation of FGFR1 is inhibited by cycloheximide, suggesting that newly synthesized cytoplasmic FGFR1, rather than old cell surface FGFR1, is translocated to the nucleus.

What Is the Function of Nuclear FGFR1?

The mitogenic effects of FGFs acting intracellularly have been shown by a number of laboratories (Imamura *et al.*, 1990; Wiedlocha *et al.*, 1994; Bikfalvi *et al.*, 1995; Ray *et al.*, 1995; Lin *et al.*, 1996; see INTRODUCTION). The presence of functional FGFR1 within the nucleus shown in the present study offers a mechanism by which these effects could occur.

Our data indicate that the majority of nuclear FGFR1 is found in a patchy distribution within the nuclear

matrix, suggesting that its function may be associated with specific regions of nuclear matrix. The nuclear matrix consists of the web of internal fibers connected to the nuclear lamina and the lamina itself (He *et al.*, 1990). DNA replication (Berezney and Coffey, 1974; McCready *et al.*, 1980), transcription (Jackson and Cook, 1985), and RNA processing (Zeitlin *et al.*, 1987) are architecturally organized on the matrix. Topoisomerase, transcriptional factors (Eisenman *et al.*, 1985; Chatterjee and Flint, 1986; Waitz and Loidl, 1991), and proteins that regulate the cell cycle (Chatterjee and Flint, 1986; Deppert and Non Der Weth, 1990; Greenfield *et al.*, 1991; Mancini *et al.*, 1994) associate with the nuclear matrix. Therefore, our findings raise the intriguing possibility that FGFR1 may exert its influence over a number of cellular processes by acting within the environment of the nuclear matrix. Several nuclear proteins coimmunoprecipitate with FGFR1 and become phosphorylated when subjected to an in vitro kinase assay. Those proteins could represent nuclear targets for FGFR1. Identification of these targets should increase our understanding of how FGF-2 and other growth factors control long-term biological processes.

ACKNOWLEDGMENTS

We thank Dr. Leslie Tolbert and Mrs. Patty Jansma (University of Arizona) for their assistance with confocal microscopy and Mr. David Bentley (University of Arizona) for his assistance with electron microscopy. We also thank Enrique Chang (Microscope System Division of Carl Zeiss, Incorporated, Thornwood, NY) for enabling us to use the LSM410 confocal system. This study was supported by the National Institutes of Health (HL-49376-01A1), National Science Foundation (94-11226), and American Parkinson Disease Association (M.K.S.). P.A.M. was supported by the National Institutes of Health (DK-18811 and NS-28121).

REFERENCES

Abraham, J.A., Mergia, A., Whang, J.L., Tumolo, A., Friedman, J., Hjerrild, K.A., Gospodarowicz, D., and Fiddes, J.C. (1986a). Nucleotide sequence of a bovine clone encoding the angiogenic protein basic fibroblast growth factor. Science *233*, 545–548.

Abraham, J.A., Whang, J.L., Tumolo, A., Mergia, A., Friedman, J., Gospodarowicz, D., and Fiddes, J.C. (1986b). Human basic fibroblast growth factor: nucleotide sequence and genomic organization. EMBO J. *5*, 2523–2528.

Allen L.E., and Maher, P.A. (1993). Expression of basic fibroblast growth factor and its receptors in an invasive bladder carcinoma cell line. J. Cell. Physiol. *155*, 368–375.

Baldin V., Roman, A.-M., Bierne, I., Almarc, F., and Bouche, G. (1990). Translocation of the bFGF to the nucleus is G1 phase cell cycle-specific in bovine aortic endothelial cells. EMBO J. *9*, 1511–1517.

Beato, M. (1989). Gene regulation by steroid hormones. Cell *56*, 335–344.

Berezney, R., and Coffey, D.S. (1974). Nuclear protein matrix: association with newly synthesized DNA. Science *189*, 291–292.

Bergonzoni, L., Caccia, P., Cletini, O., Sarmientos, P., and Isacchi, A. (1992). Characterization of a biologically active extracellular domain of fibroblast growth factor receptor 1 expressed in *Escherichia coli*. J. Biochem. *210*, 823–829.

Bikfalvi, A., Klein, S., Pintucci, G., Quatro, N., Mignatti, P., and Rifkin, D.B. (1995). Differential modulation of cell phenotype by different molecular weight forms of basic fibroblast growth factor: possible intracellular signaling by the high-molecular-weight forms. J. Cell Biol. *129*, 233–243.

Boarder, M.R., Plevin, R., and Marriott, D.B. (1988). Angiotensin II potentiates prostaglandin stimulation of cAMP levels in intact bovine adrenal medulla cells but not adenylate cyclase in permeabilized cells. J. Biol. Chem. *263*, 15319–15324.

Bouche, G., Gas, N., Prats, H., Baldin, V., Tauber, J.P., Teissie, J., and Amalric, F. (1987). Basic fibroblast growth factor enters the nucleolus and stimulates the transcription of ribosomal genes in ABAE cells undergoing GO–G1 transition. Proc. Natl. Acad. Sci. USA *84*, 6770–6774.

Boyle, W.T., Lampert, M.A., Li, A.C., and Baluda, M.A. (1985). Nuclear compartmentalization of the v-myb oncogene product. Mol. Cell. Biol. *11*, 3017–3023.

Bugler, B., Amalric, F., and Prats, H. (1991). Alternative initiation of translation determines cytoplasmic or nuclear translocation of basic fibroblast growth factor. Mol. Cell. Biol. *11*, 573–577.

Burwen, S.J., and Jones, A.L. (1987). The association of polypeptide hormones and growth factors with the nuclei of target cells. Trends Biochem. Sci. *April*, 159–162.

Chatterjee, P.K., and Flint, S.J. (1986). Partition of E1A proteins between soluble and structural fractions of adenovirus infected and transformed cells. J. Virol. *60*, 1018–1026.

Deppert, W., and Non Der Weth, A. (1990). Functional interaction of nuclear transport-deficient simian virus 40 large T antigen with chromatin and nuclear matrix. J. Virol. *64*, 838–846.

Dionne, C.A., Crumley, G., Bellot, F., Kaplow, J.M., Searfoss, G., Ruta, M., Burgess, W.H., Jaye, M., and Schlessinger, J. (1990). Cloning and expression of two distinct high-affinity receptors cross-reacting with acidic and basic fibroblast growth factors. EMBO J. *9*, 2685–2692.

Eisenman, R.N., Tachibana, C.Y., Abrams, H.D., and Hann, S.R. (1985). v-myc- and c-myc-encoded proteins are associated with the nuclear matrix. Mol. Cell. Biol. *5*, 114–126.

Frodin, M., and Gammeltoft, S. (1994). Insulin-like growth factor acts synergistically with basic fibroblast growth factor and nerve growth factor to promote chromaffin cells proliferation. Proc. Natl. Acad. Sci. USA *91*, 1771–1775.

Greenfield, I., Nickerson, J., Penman, S., and Stanley, M. (1991). Human papilloma virus 16 E7 protein is associated with the nuclear matrix. Proc. Natl. Acad. Sci. USA *88*, 11217–11221.

Grothe, C., and Unsicker, K. (1990). Immunocytochemical mapping of basic fibroblast growth factor in the developing and adult rat adrenal gland. Histochemistry *94*, 141–147.

Guidotti, A., and Costa, E. (1974). A role for nicotine receptors in the regulation of adenylate cyclase of adrenal medulla. J. Pharmacol. Exp. Ther. *189*, 665–675.

Hanneken, A., Maher, P.A., and Baird, A. (1995). High-affinity immunoreactive FGF receptors in the extracellular matrix of vascular endothelial cells—implications for the modulation of FGF-2. J. Cell Biol. *128*, 1221–1228.

He, D.C., Nickerson, J.A., and Penman, S. (1990). Core filaments of the nuclear matrix. J. Cell Biol. *110*, 569–580.

Hopkins, C.R. (1994). Internalization of polypeptide growth factor receptors and the regulation of transcription. Biochem. Pharmacol. *47*, 151–154.

Hou, J., Kan, M., McKeehan, K., McBride, G., Adams, P., and McKeehan, W.L. (1991). Fibroblast growth factor receptors from liver vary in three structural domains. Science *251*, 665–668.

Imamura, T., Engelka, K., Zhan, X., Tokita, Y., Forough, R., Roeder, D., Jackson, D., Maier, J.A.M., Hla, T., and Maciag, T. (1990). Recovery of mitogenic activity of a growth factor mutant with a nuclear translocation sequence. Science *249*, 1567–1570.

Jackson, D.A., and Cook, P.R. (1985). Transcription occurs at the nucleoskeleton. EMBO J. *4*, 919–925.

Jans, D.A. (1994). Nuclear signaling pathways for polypeptide ligands and their membrane receptors. FASEB J. *8*, 841–847.

Jaye, M., Howk, R., Burgess, W.H., Ricca, G.A., Chiu, I.-M., Ravera, M.W., O'Brien, S.J., Modi, W.S., Maciag, T., and Drohan, W.N. (1986). Human endothelial cell growth factor: cloning, nucleotide sequence, and chromosome localization. Science *233*, 543–545.

Jiang, L.-W., and Schindler, M. (1990). Nucleocytoplasmic transport is enhanced concomitant with nuclear accumulation of epidermal growth factor (EGF) binding activity in both 3T3-1 and EGF receptor-reconstituted NR-6 fibroblasts. J. Cell Biol. *110*, 559–568.

Johnson, D.E., and Williams, L.T. (1993). Structural and functional diversity in the FGF receptor multigene family. Adv. Cancer Res. *60*, 1–41.

Johnston, C.L., Cox, H.C., Gomm, J.J., and Coombes, R.C. (1995). Fibroblast growth factor receptors (FGFRs) localize in different cellular compartments. A splice variant of FGFR-3 localizes to the nucleus. J. Biol. Chem. *270*, 30643–30650.

Keegan, K., Johnson, D.E., Williams, L.T., and Hayman, M.J. (1991). Isolation of additional member of the fibroblast growth factor receptor family, FGFR-3. Proc. Natl. Acad. Sci. USA *88*, 1095–1099.

LaCasse, E.C., and Lefebvre, Y.A. (1995). Nuclear localization signals overlap DNA- or RNA-binding domains in nuclei acid-binding proteins. Nucleic Acids Res. *23*, 1647–1656.

Lin, Y-Z., Yao, S.Y., and Hawiger, J. (1996). Role of the nuclear localization sequence in fibroblast growth factor-1–stimulated mitogenic pathways. J. Biol. Chem. *271*, 5305–5308.

Lobie, P.E., Wood, T.J.J., Chen, C.M., Waters, M.J., and Norstedt, G. (1994). Nuclear translocation and anchorage of the growth hormone receptor. J. Biol. Chem. *269*, 31735–31746.

Maher, P.A. (1991). Tissue-dependent regulation of tyrosine kinase activity during embryonic development. J. Cell Biol. *112*, 955–963.

Mancini, M.A., Shan, B., Nickerson, J.A., Penman, S., and Lee, W.H. (1994). The retinoblastoma gene product is a cell cycle-dependent, nuclear matrix-associated protein. Proc. Natl. Acad. Sci. USA *91*, 418–422.

Mason, I.J. (1994). The ins and outs of fibroblast growth factors. Cell *78*, 547–552.

McCready, S.J., Goodwin, J., Mason, D.W., Brazell, I.A., and Cook, P.R. (1980). DNA is replicated at the nuclear cage. J. Cell Sci. *46*, 365–386.

Moscatelli, D. (1987). High- and low-affinity binding sites for basic fibroblast growth factor on cultured cells: absence of a role for low-affinity binding in the stimulation of plasminogen activator production by bovine capillary endothelial cells. Cell Physiol. *131*, 123–130.

Moscatelli, D. (1988). Metabolism of receptor-bound and matrix-bound basic fibroblast growth factor by bovine capillary endothelial cells. J. Cell Biol. *107*, 753–759.

Nakanishi, Y., Kihara, K., Mizuno, K., Masamune, Y., Yoshitake, Y., and Nishikawa, K. (1992). Direct effect of basic fibroblast growth factor on transcription in cell-free system. Proc. Natl. Acad. Sci. USA *89*, 5216–5220.

Partanen, J., Makela, T.P., Eerola, E., Korhonen, J., Hirvonen, H., Claesson-Welsh, L., and Alitalo, K. (1991). FGFR-4, a novel acidic fibroblast growth factor receptor with a distinct expression pattern. EMBO J. *10*, 1347–1354.

Podlecki, D.A., Smith, R.M., Kao, M., Tsai, P., Huecksteadt, T., Brandenburg, D., Lasher, R.S., Jarett, L., and Olefsky, J.M. (1987). Nuclear translocation of the insulin receptor. J. Biol. Chem. *262*, 3362–3368.

Prudovsky, I., Savion, N., Zhan, X., Friesel, R., Xu, J., Hou, J., McKeehan, W.L., and Maciag, T. (1994). Intact and functional fibroblast growth factor (FGF) receptor-1 trafficks near the nucleus in response to FGF-1. J. Biol. Chem. *269*, 31720–31724.

Puchacz, E., Stachowiak, E.K., Florkiewicz, R., Lukas, R.J., and Stachowiak, M.K. (1993). Basic regulates tyrosine hydroxylase and proenkephalin mRNA levels in adrenal chromaffin cells. Brain Res. *610*, 39–52.

Rakowicz-Szulczynska, E.M., Otwiaska, D., Rodeck, U., and Koprowski, H. (1989). Epidermal growth factor (EGF) and monoclonal antibody to cell EGF surface receptor bind to the same chromatin receptor. Arch. Biochem. Biophys. *268*, 456–464.

Ray, J., Hogg, J., Beutler, A.S., Takayama, H., Baird, A., and Gage, F. (1995). Expression of biologically active basic fibroblast growth factor by genetically modified rat primary skin fibroblasts. J. Neurochem. *64*, 503–513.

Ruta, M., Burgess, W., Givol, D., Epstein, J., Neiger, N., Kaplow, J., Crumley, G., Dionne, C., Jaye, M., and Schlessinger, J. (1989). Receptor for acidic fibroblast growth factor is related to the tyrosine kinase encoded by the *fms*-like gene (FLG). Proc. Natl. Acad. Sci. USA *86*, 8722–8726.

Scatchard, G. (1949). The attractions of proteins to small molecules and ions. Ann. NY Acad. Sci. *51*, 660–672.

Schreiber, E., Mathias, P., Muller, M.M., and Schaffner, W. (1989). Rapid detection of octamer binding proteins with "mini-extracts" prepared from a small number of cells. Nucleic Acids Res. *17*, 6419.

Schubert, D., Ling, N., and Baird, A. (1987). Multiple influences in a heparin-binding growth factor on neuronal development. J. Cell Biol. *104*, 635–643.

Schweigerer, L., Neufeld, G., Mergia, A., Abraham, J.A., Fiddes, J.C., and Gospodarowicz, D. (1987). Basic fibroblast growth factor in human rhabdomyosarcoma cells: implications for the proliferation and neovascularization of myoblast-derived tumors. Proc. Natl. Acad. Sci. USA *84*, 842–846.

Sherman L., Stocker, K.M., Morrison, R., and Ciment, G. (1993). Basic fibroblast growth factor (bFGF) acts intracellularly to cause the transdifferentiation of avian neural crest-derived Schwann cell precursors into melanocytes. Development *118*, 1313-1326.

Silver, P.A. (1991). How proteins enter the nucleus. Cell *64*, 489–497.

Stachowiak, M.K., Hong, J.S., and Viveros, O.H. (1990). Coordinate and differential regulation of phenylethanolamine *N*-methyltransferase, tyrosine hydroxylase, and proenkephalin mRNA levels in cultured bovine adrenal chromaffin cells by neural and hormonal factors. Brain Res. *510*, 227–288.

Stachowiak, M.K., Maher, P.A., Joy, A., Mordechai, E., and Stachowiak, E.K. (1966). Nuclear localization of functional FGF receptor-1 in human astrocytes suggests a novel mechanism for growth factor action. Mol. Brain Res. *38*, 161–165.

Stachowiak, M.K., Moffett, J., Joy, A., Puchacz, E., Florkiewicz, R., and Stachowiak, E.K. (1994). Regulation of bFGF gene expression and subcellular distribution of bFGF protein in adrenal medullary cells. J. Cell Biol. *127*, 203–223.

Stemple, D.L., Mahanthappa, N.K., and Anderson, D.J. (1988). Basic FGF induces neuronal differentiation, cell division, and NGF dependence in chromaffin cells: a sequence of events in sympathetic development. Neuron *1*, 517–525.

Tischler, A.S., Riseberg, J.C., Hardernbrook, A.M., and Van Cherington. (1993). Nerve growth factor as a potent inducer of proliferation and neuronal differentiation for adult rat chromaffin cells in vitro. J. Neurosci. *13*, 1533–1542.

Unsicker, K., and Westermann, R. (1992). Basic fibroblast growth factor promotes transmitter storage and synthesis in cultured chromaffin cells. Dev. Brain Res. *56*, 211–216.

Vlodavsky, I., Bar-Shavit, R., Ishai-Michaeli, R., Bashkin, P., and Fuks, Z. (1991). Extracellular sequestration and release of fibroblast growth factor: a regulatory mechanism? Trends Biochem. Sci. *16*, 268–271.

Waitz, W., and Loidl, P. (1991). Cell cycle-dependent association of c-myc protein with the nuclear matrix. Oncogene *6*, 29–35.

Wiedlocha, A., Falnes, P.O., Madshus, I.H., Sandvig, K., and Olsnes, S. (1994). Dual mode of signal transduction by externally added acidic fibroblast growth factor. Cell *76*, 1039–1051.

Wilkie, A.O.M., Morriss-Kay, G.M., Jones, E.Y., and Heath, J.K. (1995). Functions of fibroblast growth factors and their receptors. Curr. Biol. *5*, 500–507.

Xu, J., Nakahara, M., Crabb, J.W., Shi, E., Matuo, Y., Fraser, M., Kan, M., Hou, J., and McKeehan, L.W. (1992). Expression and immunochemical analysis of rat and human fibroblast growth factor receptor (flg) isoforms. J. Biol. Chem. *267*, 17792–17803.

Yamamori, T. (1990). Molecular mechanisms for generation of neural diversity and specificity: roles of peptide factors in development of postmitotic neurons. Neurosci. Res. *12*, 548–582.

Zeitlin, S., Parent, A., Silverstein, S., and Efstratiadis, A. (1987). Pre-mRNA splicing and the nuclear matrix. Mol. Cell. Biol. *7*, 111–120.